RAPPORTSERIE

Nr. 32 - Oslo 1986

BERT RUDELS:

Estimating the exchanges through the Fram Strait by classical methods: Hydrography , TS-analysis and minimizing techniques

NORSK POLARINSTITUTT

Nr. 32 - Oslo 1986

BERT RUDELS:

Estimating the exchanges through the Fram Strait by classical methods: Hydrography , TS-analysis and minimizing techniques

Bert Rudels
Norsk Polarinstitutt
Rolfstangveien 12
1330 Oslo Lufthavn

Abstract

The mass transports through the Fram Strait are determined by requiring that the total geostrophic flow field should be one of minimum kinetic energy and be subject to given constraints on the total exchanges and on the deep water circulation. To obtain the required constraints the transports through the other passages have to be estimated, and the deep water exchanges evaluated from θ-S analysis of the deep water masses in the different basins of the Arctic Mediterranean and some assumptions on the Bering Strait inflow.

The obtained transports are lower than those usually presented for the Fram Strait and show large qualitative if not quantitative differenc from year to year. It is especially clear that a variational approach, which combine synoptic section with constraints derived from yearly averaged conditions can lead to distorted solutions.

1. Introduction

The Fram Strait, the deepest and presumably the most important connection between the Arctic Ocean and the world oceans, has recently become an area of growing scientific interest and research. Studies have been made on the transports of mass and heat through the strait, on the properties of the passing water masses and on the processes active in the area.

In this work we shall try to estimate the mass transports through the strait from hydrographic sections taken across the passage. The velocity field is assumed to be geostrophic and the "level of no motion" is determined by a variational approach, in which the total kinetic energy $\frac{1}{2}\int\rho v^2 dxdz$ is minimized subject to given auxilary constraints.

As constraints we shall use mass and salt continuity for the entire Polar Ocean, and a separate estimate of the strength of the deep water exchanges by a study of the θ-S structures in the different northern basins.

The derivation of the deep water constraints demands a fairly thorough discussion of the water masses and the processes present and active in the northern seas and will fill a major part of this note.

In section 2 the hydrographic structure in the strait is discussed and in section 3 the constraints are derived. The variational approach is introduced in section 4 and the obtained flow field and transports are presented and evaluated in section 5. Finally in section 6 some suggestions for future work are given. The work is presented in more detail in Rudels 1986a,b,c, where also fuller references are given.

2. The hydrography of Fram Strait

We shall discuss two hydrographic sections, one taken from H.M.S. YMER in August 1980 and the other from M/S LANCE in August 1983. The 1983 section runs in the eastern part of the strait half a degree to the north of the YMER section and across the Molloy Deep. The quality of the LANCE section is somewhat worse than that of the YMER section, but it should be workable. The two sections have been intercalibrated by requiring the same salinity of the Greenland Sea deep water (GSDW) on the two cruises.

The quality of the data then leaves much to be desired but the differences in θ-S characteristics of the water masses are large enough to be detected in the data, and sections should be acceptable for estimating the transports.

Two features are readily noticed, when the two sections are compared.

1) The similar structures of the temperature and salinity fields on the

two sections.

2) The warmer and more saline Atlantic water present in 1983 as compared to 1980.

The first feature structure suggests a permanence of the flow and makes an effort to determine the flow field from hydrographic data more justified.

Otherwise the sections reveal the expected picture (Figs. 1,2). Polar surface water is present on almost the entire cross section, overriding the Atlantic water to the east as a thin surface layer, which gradually thickens towards the west and almost completely dominates the water column on the Greenland shelf. Atlantic water is found as a 500-700 m thick layer in the upper parts of the sections. Its distribution suggests two distinct cores. The eastern core is found further to the west in 1980 than in 1983, while the position of the western core appears to be the same on the two sections. There are weak east-west gradients in temperature and salinity, which implies that the western core may represent Atlantic water moving south after a brief recirculation in the northern vicinity of the strait (see sect. 5 below).

Close to the Greenland continental slope these horizontal gradients become stronger and west of the front the Atlantic water has become considerably cooler and fresher (provided that the designation Atlantic water can be used for all waters with $T > 0^0 C$, $S > 34.7$). Anticipating results and conjectures to be derived below we believe that the cold, less saline Atlantic water to the west represents an outflow from the interior of the Polar Ocean.

In the deeper layers the direction of the horizontal temperature and salinity gradients have changed and the warmer more saline water is now found to the west. This reversal of the property distributions as compared to the upper layers is in agreement with an outflow of saline polar dominated deep water to the west and the presence of fresher, colder deep water from the Greenland/Norwegian Seas in the eastern part. However, the water column in the western part shows strong interleaving between colder, fresher and warmer, saltier water masses in the deeper parts as well as in the Atlantic layer, suggesting that a northward flow of GSDW may take the place also on the western side of the passage.

To simplify the discussion of water mass transports and transformations we introduce 6 water masses largely based upon the classification by Swift and Aagaard (1981) (see Table I) and the distribution of these waters on the sections are shown in Figs. (3a,b). The deep water has been further subdivided to separate the Polar Ocean and the Greenland/Norwegian Seas deep waters. The water mass distribution is further clarified by θ-S diagrams from the different parts of the sections (Fig. 4).

Table I

Water masses

Water mass	Temperature range	Salinity range
I	$\theta < 0$	$S < 34.7$
II	$0 < \theta$	$S < 34.5$
IIa	$0 < \theta < 1$ $1 < \theta$	$34.5 < S < 34.7$ $34.5 < S < 34.9$
III	$\theta < 0$	$34.7 < S$
IV	$0 < \theta < 1$	$34.7 < S$
V	$1 < \theta < 3$	$34.9 < S$
VI	$3 < \theta$	$34.9 < S$

3. The Constraints

3.1. Mass and salt balances in the Polar Ocean

The transports through Fram Strait must conform to obvious (and less obvious) continuity requirements and we shall try to estimate and use some of these requirements as constraints on the geostrophic velocity field.

Two necessary demands are that mass and salt balances should hold for the entire Polar Ocean. If the exchanges through the other passages; The Arctic Archipelago, the Barents Sea and the Bering Strait as well as the freshwater supply and the ice export were known, the net transports through Fram Strait could be determined. However, these exchanges are not established with any excessive certainty. The Bering Strait inflow is probably the best known (Coachman & Aagaard 1981), while the knowledge of the transports through the Barents Sea and the Arctic Archipelago is far from satisfactory. The ice export has been revised upwards in the last few years (Vinje & Finnekåsa 1986; Östlund & Hut 1984). The river run off should be well known but the results reported by Östlund & Hut throw some doubts on the most cited figure (0.1 Sv.). Be that as it may, in Table II we summarize the values used in this work. The details are found in Rudels (1986a,b).

However, mass and salt balances are not enough. The freshening of the surface water and the Atlantic layer and the increased salinity in the deeper parts indicate that two processes are active in the Polar Ocean. One dilutes the surface layer and thus drives an estuarine circulation, while the other creates dense salty water, which sinks down and influences the deeper parts. This implies that the outflow is both fresher - at the surface - and saltier - in the deeper layers -, than the corresponding inflows. If any minimizing process is applied to such a configuration using only mass and salt continuity, the solution will be one of two superposed opposing gyres (Rudels 1986a). The upper gyre transports Atlantic water into the Polar Ocean and exports low saline polar surface water, while the lower gyre drives the saline deep water into the Polar Ocean and forces the fresher deep water southwards, contrary to our knowledge of the water mass distribution in the Arctic Mediterranean (see below, and Aagaard et al. 1985; Rudels 1986c).

3.2. The θ-S structure in the deep layers

To prevent this to happen, some constraints must be imposed on the deep circulation, and we have to examine more carefully the θ-S structures in the Norwegian Sea, the Fram Strait, the Polar Ocean and the Greenland Sea. The data are taken from the cruise with M/S POLARSIRKEL

in the Greenland Sea in April 1980 and from the YMER cruise in the summer 1980. The stations are shown in Fig. 5.

The θ-S structure of the deeper layers ($\theta < 0$) on the Svalbard continental slope and west of the Yermak plateau is tight, clearly defined and resembles that observed further to the south in the Norwegian Sea (Figs. 6a,b,c). In the central area of the Fram Strait θ-S structure is more diffuse, colder and fresher, indicating the additional presence of GSDW (Fig. 6d). The active interleaving is mostly confined to the strait and the water column in the interior of the Polar Ocean (north of Frans Josef Land) again shows a tight, characteristic θ-S structure quite different from the one found in the Norwegian Sea. The salinity has increased slightly in the upper and rather dramatically in the deeper parts and the water column exhibits a salinity maximum at the bottom. The potential temperature is there around -0.96 (Fig. 6e).

In the outflow region in the western Fram Strait an additional salinity maximum is present higher up in the water column (at $\theta \sim -0.5$), while the deeper maximum is still present (Fig. 6f).

In the Greenland Sea the water transformations appear to be different on the continental slope and in the central gyre. On the slope the upper salinity maximum is gradually reduced but still present (Fig. 6g), while in the central Greenland Sea this upper maximum is absent and the lower maximum has become weaker, colder and is no longer found close to the bottom but above the colder fresher Greenland Sea bottom water (Fig. 6h).

These changes show that processes are active not only in the Greenland Sea but also in the Polar Ocean, which transform the surface water and make it sink down into and affect the deeper layers. Most of the changes of the deep water θ-S structure are density compensating and an increase of salinity is usually accompanied by an increase in temperature.

The most effective way to increase the density of the surface water is by brine rejection due to freezing. In the Polar Ocean this process is favoured by the shallow shelves, which allow the saline water to accumulate and reach the high densities, which may bring it down into the deeper layers as it subsequently leaves the shelf.

In the Greenland Sea no lower boundary is present and only a small density increase may occur before the particles leave the surface layer to merge with the underlying waters. The higher salinity of the Polar Ocean deep water (PODW) as compared to the GSDW supports such a view.

However, this cannot be the whole story, since the ice formation requires that the transformed water is at the freezing point contrary to what is observed. The interaction with the intermedieate water masses must be taken into account. In the Polar Ocean the dense shelf water will sink through and entrain the warmer and less saline

Atlantic water, which will increase the temperature and lower the salinity of the shelf contribution. In the Greenland Sea the dense surface water passes through cold but more saline intermediate water and gradually becomes warmer and more saline and approaches the θ-S characteristics of the Greenland Sea bottom water from below (in the θ-S diagram).

These convective contributions of surface and entrained waters then merge into the deep waters. In the steady state, which we assume exists, the influences of convective contributions must, to maintain the θ-S structures, be balanced by advective inflows from the neighbouring basins. The transformed deep water is then exported and becomes the advective contribution to the next basin.

A scenario for the deep water circulation would then be somewhat like this; An inflow of Norwegian Sea deep water (NSDW) takes place through the Fram Strait. It is augmented by shelf water and entrained intermediate water in the Eurasian basin. The flow then splits due to the Lomonosov ridge, which prevents the deeper layers from entering the Canadian basin. In the Canadian basin a further convective contribution is introduced and the Canadian basin deep water (CBDW) then reenters the Eurasian basin, mixes with the Eurasian basin deep water (EBDW) in the thermodynamically inactive area north of Greenland to form the PODW and supplies the upper of the two characteristic salinity maxima of the PODW. THE PODW then splits after passing through the Fram Strait and one part follows the continental slope while the other part enters directly into the Greenland Sea.

To parameterize the mixing on the slope we replace the part of the polar deep water outflow which enters the Greenland Sea with an equal amount of GSDW. One part of the PODW then form the advective component in the Greenland Sea column, while the mixing of the PODW and the GSDW on the slope creates a water mass, which is advected across the southern part of the Greenland Sea into the Norwegian Sea to form the NSDW.

This is essentially the scenario of Aagaard & et al. (1985) and also discussed in Rudels (1986c).

3.3. The active processes

We shall now try to assess the different contributions and estimate the strength of the deep circulation from the θ-S characteristics. Needless to say the estimate will be subjective and uncertain, but we believe that such an exercize is worthwhile.

Starting in the Canadian basin we notice that the advective contribution to the deep water is the part of the water column in the Eurasian basin, which lies above the sill depth of the Lomonosov ridge. However, the water inside the Canadian basin is warmer and more saline than the waters at the sill depth in the Eurasian basin (Coachman & Aagaard 1974). The Atlantic layer by contrast has become cooler

and fresher. The two water columns are sketched in Fig. 7. The added convective water mass, which is the cause of this transformation, is a mixture of brine enriched water at the freezing point from the shelves and water entrained from the intermediate layers as the shelf water descends as plumes through the water column.

If we knew the salinity and the formation rate of the shelf waters and had a reliable theory for entraining buoyant plumes on a sloping boundary in a stratified, rotating system, the gradual evolution of the θ-S characteristics of the plume could be computed. This is, however, presently not the case. Instead we have tried to indicate the θ-S characteristics of the terminal points of the plumes as they reach their optimal density level. It should perhaps be pointed out that the plumes do not evolve along these indicated points but instead approach the curve from beneath as they become diluted by the intermediate water masses (Fig. 7).

The curve has not been drawn completely at random. As our starting point we have taken into account that the deep water in the Canadian basin and the densest water entering across the Lomonosov ridge have equal density. This indicates that the CBDW is the result of an isopycnal mixing between the advective and convective contributions. To find the ratio of shelf water to entrained water we have approximated the θ-S characteristics of the intermediate waters with those of the Atlantic layer and connected these to the θ-S characteristics of the shelf water to be found along the line of freezing on the θ-S diagram.

The mixing ratio of the entrained water to shelf water could conceivably range from more than 5 to less than 1/2. However, the convective contribution have to mix with the deep water from the Eurasian basin to form the CBDW and too saline shelf water (line A) would imply a large component of Atlantic water and a still larger inflow of EBDW. Too fresh shelf water (line B) would on the other hand give a somewhat less Atlantic inflow and almost no contribution from the EBDW. We expect the advected amount of Atlantic water and EBDW to be of equal magnitude, which suggests a ratio of 1:1 between the advected and convected contributions (line C). The ratio of entrained water to shelf water then becomes 2:1 and the salinity of the shelf water should be around 35.1. Aagaard et al. (1985) have arrived at the same estimate by a somewhat different argumentation. We would expect the same ratio 2:1 between entrained intermediate water and shelf water to hold for the descending plumes also in the Eurasian basin. The advective contribution is in this case the NSDW and the θ-S diagram here indicates a larger advective to convective contribution - 8:1 - for the Eurasian basin. This makes sense considering the proximity to the inflow area in the Fram Strait (Fig. 8). Another reason for the small convective contribution is that a substantial fraction of the entrained water is deep water, which does not add to the convective water mass, but only redistribute the characteristics of the

deep water.

Ice formation is not generally accepted as the ultimate cause of the deep ventilation of the central Greenland Sea, but to our mind the θ-S structures encountered there are most readily explained by a mixing between a cold, fresh water mass lying horizontally just above the freezing point line in the θ-S diagram, as would be the case with cold plumes and thermals sinking from the surface, and a vertically oriented water mass with temperature ranging between 0 and -1^0 and a rather high salinity, that is, the Polar Ocean deep water (Rudels 1986c).

However, in the absence of a shallow physical boundary no high salinities can be reached at the surface in the Greenland Sea and the dense water formed at the sea surface therefore gives the GSDW a cool and fresh signature. Due to the absence of intermediate water masses in the Greenland Sea the entrainment only results in a redistribution of the deep water and the convective contribution is taken to be equal to the water leaving the surface. The ratio of convective and advective contributions to the GSDW is estimated to be 1:2 (Fig. 9).

We do not consider any contributions from the Atlantic water to enter the GSDW either by direct cooling or by double-diffusive convection. The salinity maximum ($\theta \sim -1.1$, $S \sim 34.90$) at 2000 m is more easily interpreted as a remnant of the deep PODW salinity maximum than as a sign of Atlantic water.

We have now examined the active areas of the Arctic Mediterranean, but so far not commented on the pure mixing zones; The outflow area north of Fram Strait, where the EBDW and the CBDW meet, and the Greenland slope, where PODW and GSDW mix to form NSDW. Again we have to rely on subjective interpretations of the θ-S diagrams (Figs. 9,10) and we have settled for the ratios 2:1 of EBDW to CBDW to make PODW and 1:1 of PODW to GSDW to make NSDW.

The relative contributions to the different water masses are listed in Table (III).

3.4. Quantitative estimates of the deep circulation

The results of this lengthy discussion will now be used to estimate magnitude of the deep circulation. Assuming an inflow of X Sv. NSDW to the Polar Ocean, this is augmented by 0.125X Sv. in the Eurasian basin. The deep water then splits, Y Sv. enters the Canadian basin, where another volume Y Sv. is added before the CBDW reenters to merge with the remaining (1.125X - Y) Sv. of EBDW. Since the PODW consists of twice as much EBDW as CBDW we have $4Y = 1.25x - Y$ and the PODW outflow becomes $(1.125X + Y) = 1.4X$. The water added to the deeper layers in the Polar Ocean is then about half of the inflow through the Fram Strait.

Since we have assumed that half of this outflowing water on the

Table II

Different contributions to the Arctic Ocean mass, heat and salt balances

Passage	Mass transport 10^9 kg/s	Temp. ^{0}C	Heat transport * 10^9 kcal/s	Sal.	Salt transport 10^6 kg/s
Bering Strait					
Summer Water	0.6	5	3.0	32.4	19.44
Winter Water	0.2	-1.8	-0.36	32.4	6.48
Ice	0.005	-1.8	-0.40		
Arctic Archipelago					
Surface Water	-0.7	-1.0	0.7	32.9	-23.03
Deep Exchange	-0.3	-0.5	0.15	34.3	-10.29
Barents Sea					
Coastal Water	0.8	-1.8	-1.44	34.85	27.88
Atlantic Water	0.4	1.0	0.4	35.05	14.02
Run off	0.10	5	0.5	-	-
Net. precip.	0.02	-	-	-	-
Ice export	0.08	-1.8	6.54	3.0	0.24
total transport	1.04		8.3		34.74

* Transport relative to 0^0C

Table III

Ratio of contributions making up the different deep waters

	advective/convective
Canadian basin DW	1:1
Eurasian basin DW	8:1
Greenland Sea DW	2:1
Polar Ocean outflow	Can DW / Eur DW 1:2
Norwegian Sea DW	PODW / GSDW 1:1

Table IV

Transports through the Fram Strait

Exchanges through the Fram Strait (YMER section case II)

	mass transport 10^9 kg/s		heat transport 10^9 kcal/s	
West Spitsbergen Current				
AW	1.9		5.4	
DW	1.1		-1.0	
East Greenland Current				
PSW	-0.9		1.26	
AW	-1.0	-2.6	-1.73	-0.8
MAW	-0.7		-0.34	
DW	-1.5		0.8	
ice	-0.08		6.4	
net transport	-1.1		4.4	(excl. ice)

slope is exchanged for GSDW, 0.7X PODW enters the Greenland Sea, thus requiring a deep water formation of 0.35X in the central Greenland Sea gyre to maintain a stationary θ-S structure in the Greenland Sea.

We then have a net production of deep water of 0.8X Sv. in the northern basins, which must leave the deep water sphere either by definition (get warmed above 0^0) or flow south into the North Atlantic. Our personal belief is that the excess water passes south across the Icelandic Sea into the North Atlantic. However, this means that a large amount of PODW leaves the circulation and that the inflow to the Polar Ocean should then have a correspondingly larger contribution from the Greenland Sea. Something, which does not seem warranted from the θ-S diagrams (Fig. 10), but it could be the case if an inflow of GSDW occurs further to the west in Fram Strait.

Considering the level of accuracy maintained in this discussion this issue is of small importance.

The θ-S diagram cannot guide us any further and we have to make some guesses to estimate X. We have assumed that the dense water on the shelves in the Canadian basin is formed from Bering Sea water and that 10% or about 0.08 Sv. (Table II) of the inflow through the strait is transformed to dense shelf water. Y then becomes 0.24 Sv., which gives X = 1.1 Sv. 1.1 Sv. NSDW thus enters and 1.4 Sv. PODW leaves the Polar Ocean. The corresponding average salinities are estimated from the θ-S diagrams to be 34.905 and 34.925 respectively.

A more extensive if perhaps not more accurate discussion of the deep water circulation is given in Rudels (1986c).

We have at last obtained two additional constraints to be applied on the deep circulation and we are ready to determine the flow field in the Fram Strait.

4. The Variational Approach

The observed density field in Fram Strait allows us to compute the geostrophic velocities up to an unknown barotropic part. We hope to determine that part by the additional requirement that the flow field should fulfil the transport constraints derived above. The number of constraints is less than the number of station pairs and the problem is underdetermined. Some rationale is therefore necessary for choosing one solution from all the possible ones, and we shall follow the variational approach outlined by Claerbout (1976) and similar to the one used by Stommel & Veronis (1980). Mathematically more sophisticated methods are, however, also available (e.g. Wunch 1978; Roemmich 1980; Fiadeiro & Veronis 1982; Wunsch & Grant 1982)

We shall look for the solution with the least <u>total</u> kinetic energy. This means that the total flow field will be independent of the ini-

tial level of no motion chosen to compute the baroclinic field and thus unique. This is but one way to deal with the uniqueness problem and we refer to Fiadeiro & Veronis (1982) for a fuller discussion.

The use of kinetic energy also automatically weights the solution so that the effects of varying cross sectional areas between the stations are removed. The integral

$$\int_A \varrho v^2 dxdz, \qquad A = \text{area of cross-section in Fram Strait}$$

is minimized subject to the constraints

$$\int_A \varrho v^b \delta_l dxdz = C_l = C_{0l} - \int_A \varrho v^{bc} \delta \, dxdz \qquad l = 1 \ldots L$$

which state that the added barotropic velocity field fulfils the continuity requirements C_{0l} introduced above except for the contributions from the already computed baroclinic field. L is the number of constraints and δ_l is a dimension factor.

Introducing the lagrangian multipliers λ_l we have

$$\frac{\partial}{\partial v^b} \{ \int_A 2^{-1} \varrho v^2 dxdz - \sum_{l=1}^{L} \lambda_l \{ \int_A \varrho v^b \delta \, dxdy - C_l \} \} = 0$$

because the baroclinic field $v^{bc}(x.z)$ is given by the density distributions and only the barotropic part $v^b(x)$ can be varied. Changing to discrete notation we get

$$\frac{\partial}{\partial v_i^b} \{ \sum_{i=1}^{N} \varrho \, 2^{-1} \, (\sum_{j=1}^{k(i)} v_{ij}^{bc} + v_i^b)^2 \} - \sum_{l=1}^{L} \lambda_l \{ \sum_{i=1}^{N} \sum_{j=1}^{k(i)} \varrho a_{ij} \delta_{ijl} v_i^b - C_l \} = 0$$

or

$$v_i^b + \sum_{j=1}^{k(i)} (\varrho a_{ij} v_{ij}^{bc}) / a_i + \sum_{l=1}^{L} \lambda_l \sum_{j=1}^{k(i)} (\varrho a_{ij} \delta_{ijl}) / a_i \qquad i = 1 \ldots\ldots N$$

where N is the number of station and each station has been divided into k(i) boxes j with area a_{ij}. $a_i = \sum_{j=1}^{k(i)} a_{ij}$ is the cross sectional area of station i.

The constraints are written as

$$\sum_{i=1}^{N} \sum_{j=1}^{k(i)} (\varrho a_{ij} \delta_{ijl}) v_i^b = C_l \qquad l = 1 \ldots\ldots L.$$

In matrix form these equations become

$$v^b + g + B\Lambda = 0$$

$$A^T v = C$$

which gives

$$v^b = B(A^TB)^{-1}C + B(A^TB)^{-1}A^Tg - g$$

The introduced constraints can be written as

$$\int_A \rho v^b(x)dxdz = M = M_0 - \int_A \rho v^{bc}(x.z)dxdz$$

$$\int_A \rho s(x.z)v^b(x)dxdz = S = S_0 - \int_A \rho s(x.z)v^{bc}(x.z)dxdz$$

$$\int_A \rho v^b(x)\Gamma(S - S_0)\Gamma(T_0 - T)dxdz = M' = M_0' - \int_A \rho v^{bc}(x.z)\Gamma(S - S_0)\Gamma(T_0 - T)dxdz$$

$$\int_A \rho s(x.z)v^b(x)\Gamma(S - S_0)\Gamma(T - T)dxdz = S' = S_0' - \int_A \rho s(x.z)v^{bc}(x.z)\Gamma(S - S_0)\Gamma(T_0 - T)dxdz$$

with $\Gamma(S - S_0) = 1 \quad S > S_0 \qquad \Gamma(T_0 - T) = 1 \quad T_0 > T$

$\Gamma(S - S_0) = 0 \quad S < S_0 \qquad \Gamma(T_0 - T) = 0 \quad T_0 < T$

which gives $C = -\begin{vmatrix} M \\ S \\ M' \\ S' \end{vmatrix}$ and M_0, S_0, M'_0, S'_0 are derived in section 2 above.

5. The Velocity Fields and the Transports

The resulting velocity fields for the two sections are shown in Fig. (12a,b). The sections superficially confirm our preconceived ideas. The inflow takes place in the eastern part, both in the Atlantic and the deeper layers. The shear is substantially weaker on the eastern side than in the outflow area to the west, where especially the strong baroclinic part of the East Greenland Current is conspiscous in the upper layers. There are several flow reversals both in the inflow and in the outflow area as would be expected from the strong eddy activity in the strait as is documented from satellite observations.

However, there is also a surprisingly strong inflow over the upper part of the Greenland slope, especially on the 1983 section. This is contrary to what we expected since the water masses in this area are most likely derived from the Polar Ocean.

To find if the flow field is consistent with the expected water mass distributions we therefore compute the integrated transports in different temperature interval as functions of salinity (Fig. 13). The lowsaline polar outflow is excluded.

These transport functions show that the inflow of deep water ($\theta < 0$) occurs at lower temperatures and salinities than the outflow. In the upper layers ($\theta > 1$) the situation is reversed and the inflows are there both warmer and saltier than the outflows. The two processes thought active in the Polar Ocean, the cooling and freshening of the upper layers and the increasing of the salinities of the deeper layers are thus mirrored in the flow field. The differences in temperature and salinity of the Atlantic water between the two years are also clearly seen.

The only serious discrepancy between the two sections is found for the transports in water mass IV ($0 < \theta < 1$, $S > 34.7$) which in 1980 indicates an outflow and in 1983 an inflow.

This water mass has two possible sources. It may represent an outflow of modified Atlantic water from the Polar Ocean and is then likely to be observed in the outflow area over the Greenland slope. It may, however, also be formed by winter cooling of Atlantic water in the Greenland Sea and then transported north towards the eastern inflow area. To the west this water mass appears as a temperature maximum, while it in the east is more of a transition layer. In 1980, however, it showed up as a salinity minimum.

So far we have not separated the transport functions for the different areas and cannot tell if we are observing a year to year variation in the relative strengths of the transports of these two waters. We therefore have to compute the transports of the water masses I-VI for different parts of the sections (Fig. 14).

These transports clearly show that in 1983 there is an inflow of water mass IV in the west contrary to what is expected, while in 1980 an outflow is found in the same area. The 1983 section also has a stronger outflow of the water masses V and VI in the western part than the corresponding inflow to the east. All this indicate that the flow field obtained for the 1983 section is, if not altogether wrong, at least seriously flawed.

Why should this be the case, and why do no such obvious contradictions appear in the 1980 section?

We believe that this feature is due to the use of average constraints, such as mass and salt balances for the Polar Ocean, together with synoptic sections in Fram Strait taken in August, when the freshwater content in the water column is at its peak. The vertical shear of the flow will increase and give a large export of low saline surface water. The system might run out of freshwater. To prevent this from happening the solution will shift the strongest outflow towards more saline stations closer to the center of the section. To maintain the salinity (or freshwater) and mass balances a low saline inflow is needed and has to occur to the west. Moreover, to diminish the freshwater export the polar surface water outflow velocities are kept low by moving the level of no motion upwards, which implies that the underlying water masses are forced to flow northward into the Polar Ocean.

Taking all this into account it is perhaps more surprising that the 1980 section looks as reasonable as it does. This is probably due to the weaker shear present in 1980, which makes it easier for the system to keep its freshwater balance.

Since the situation during most of the year is one with weaker shears, we suspect that the result for the 1980 section, apart from better conforming to our preconceived ideas, also better represents the average transports and velocities in Fram Strait than what was found for the 1983 section. However, the obtained flow field is still likely to give the main outflow displaced towards the centre of the strait.

The best we can do is just to present the results from the 1980 section with all the question marks indicated but retained (Table IV).

The northward flow of Atlantic water in the West Spitsbergen Current is rather low, 1.9 Sv., and about half of it appears to recirculate in the vicinity of the strait. The other half together with the inflow over Barents Sea make up the outflow of the modified Atlantic water and the polar surface water as well as most of the deep water formed in the Polar Ocean. The rather low outflow of modified Atlantic water indicates that the thick Atlantic layer in the Polar Ocean is ventilated at a fairly low rate, probably even lower than that of the deep waters. This impression may, however, to a large extent be due to an overestimate of the recirculation as was mentioned above.

6. Discussion

How can we proceed to improve these results? Is there any possibility to refine the method, perhaps by using sections from both summer and winter averaged separately over several years to remove short-time variabilities and the annual freshwater cycle? Would it be possible to let the freshwater cycle enter directly into the constraints? Could more tracer informations be added?

However, these improvements may not be enough and we may have to rely on direct current measurements rather than extensive hydrography to improve our transport estimates.

My own personal view is that it is time to move from approaches, which passively monitor the flow and integrate all the processes active in the system, and instead try to separate and directly estimate and model the different driving forces behind the exchanges such as:

The thermodynamic forcing of both the estuarine circulation by the freshening the Atlantic inflow and the deep circulation by brine rejection in connection with ice formation.

The wind fields, affecting the sea level slope both locally and on larger scales and thus conditioning the barotropic velocity field in the strait and also setting up wind driven transports in the strait and in the different basins.

The topography, which influences the deeper exchanges by allowing strong boundary currents to develop and thus intensify the deep exchange.

What is the relative importance of these processes, and how do they combine to determine the circulation of the Arctic Mediterranean?

References

Aagaard, K., Swift, J.H. & Carmack, E.C. 1985: Thermohaline circulation in the Arctic Mediterranean Seas. J. of Geophys. Res. 90, 4833-4846.

Claerbout, J. 1976: Fundamentals of the geophysical data processing. New York, McGraw-Hill, 274 pp.

Coachman, L. & Aagaard, K. 1974: Physical oceanography of the arctic and subarctic seas. Chapt. 1, pp. 1-72 in Herman Y. (ed.): Marine geology and oceanography of the arctic seas. New York, Springer Verlag.

Coachman, L. & Aagaard, K. 1981: Reevalution of water transports in the vicinity of Bering Strait. Pp. 95-110 in Hood, D.W. & Calder, J.A. (eds.): The Eastern Bering Sea Shelf. Oceanography and Resources, vol. 1. Dep. of Commerce/Natl. Oceanic & Atmospheric Admin, Washington D.C.

Fiadeiro, M.E. & Veronis, G. 1982: On the determination of absolute velocities in the ocean. J. of Marine Research, vol. 40, suppl., 159-182.

Roemmich, D. 1980: Estimation of meridional heat flux in the North Atlantic by inverse methods. J. of Phys. Oceanogr. 10, 1972-1983.

Rudels, B. 1986a: On the Mass Balance of the Polar Ocean, with Special Emphasis on the Fram Strait. Norsk Polarinstitutt Skrifter, in press.

Rudels, B. 1986b: The Outflow of Polar Water through the Arctic Archipelago and the Oceanographic Conditions in Baffin Bay. Polar Research, in press.

Rudels, B. 1986c: The θ-S Relations in the Northern Seas. Implications for the Deep Circulation. Polar Research, in press.

Swift, J.H. & Aagaard, K. 1981: Seasonal transitions and water mass formation in the Iceland and Greenland seas. Deep-Sea Res. 28, 1107-1129.

Tan, F.C. & Strain, P.M. 1980: The distribution of sea-ice melt water in the eastern Canadian Arctic. J. of Geophys. Res. 85, 1925-1932.

Vinje, T. & Finnekåsa, Ø. 1986: The Ice Transport through the Fram Strait. Norsk Polarinstitutt Skrifter, in press.

Wunsch, C. 1978: The North Atlantic general circulation west of 50^0W determined by inverse methods. Rev. of Geophys. and Space Phys. 11, 583-620.

Wunsch, C. & Grant, B. 1982: Towards the general circulation of the North Atlantic. Progr. in Oceanogr. 11, 1-59.

Östlund, H.G. & Hut, G. 1984: Arctic Ocean Water Mass Balance from Isotope Data. J. of Geophys. Res. 89, 6373-6381.

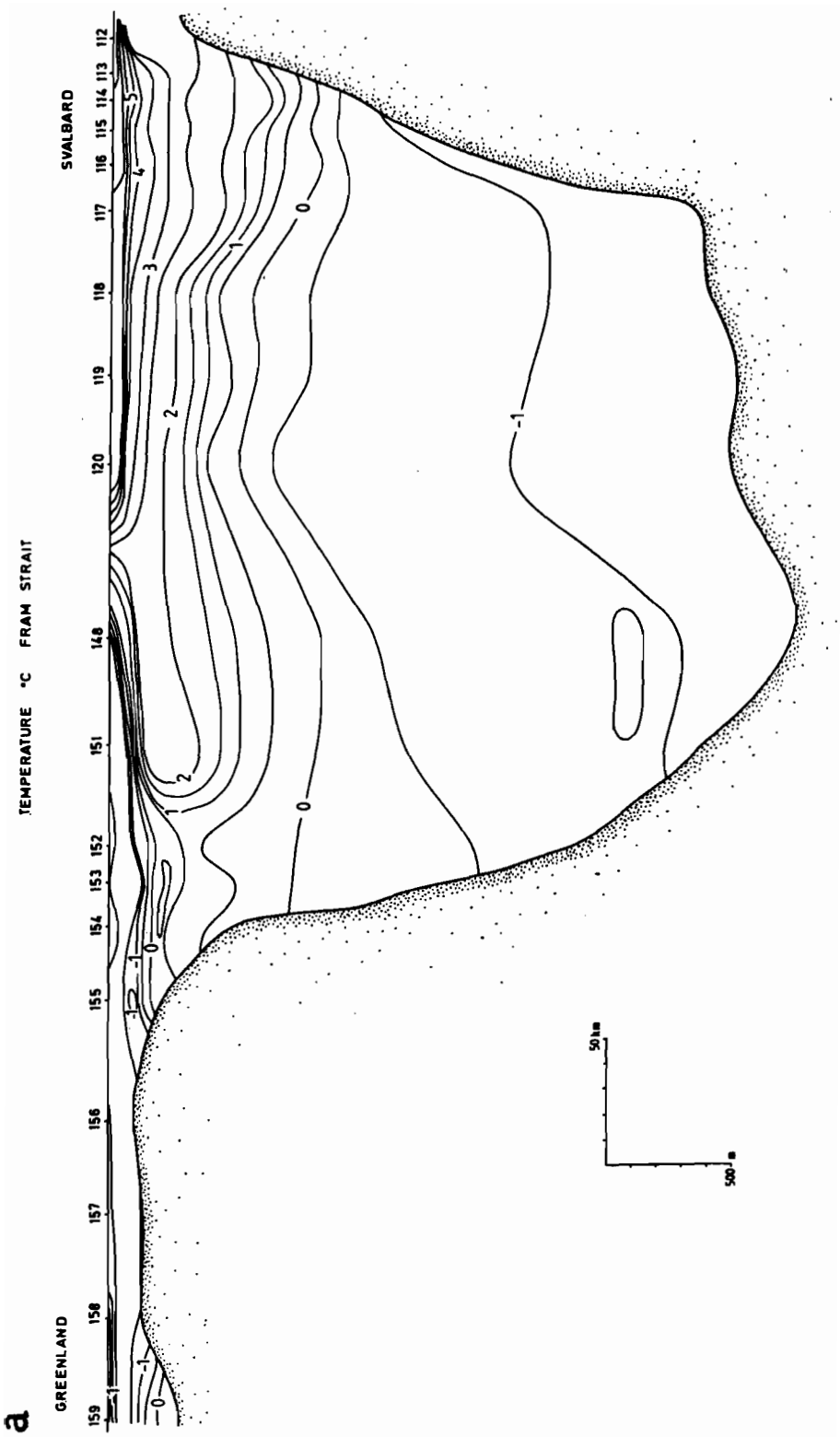

Figure 1a-c. Sections of potential temperature, salinity and potential density: YMER section.

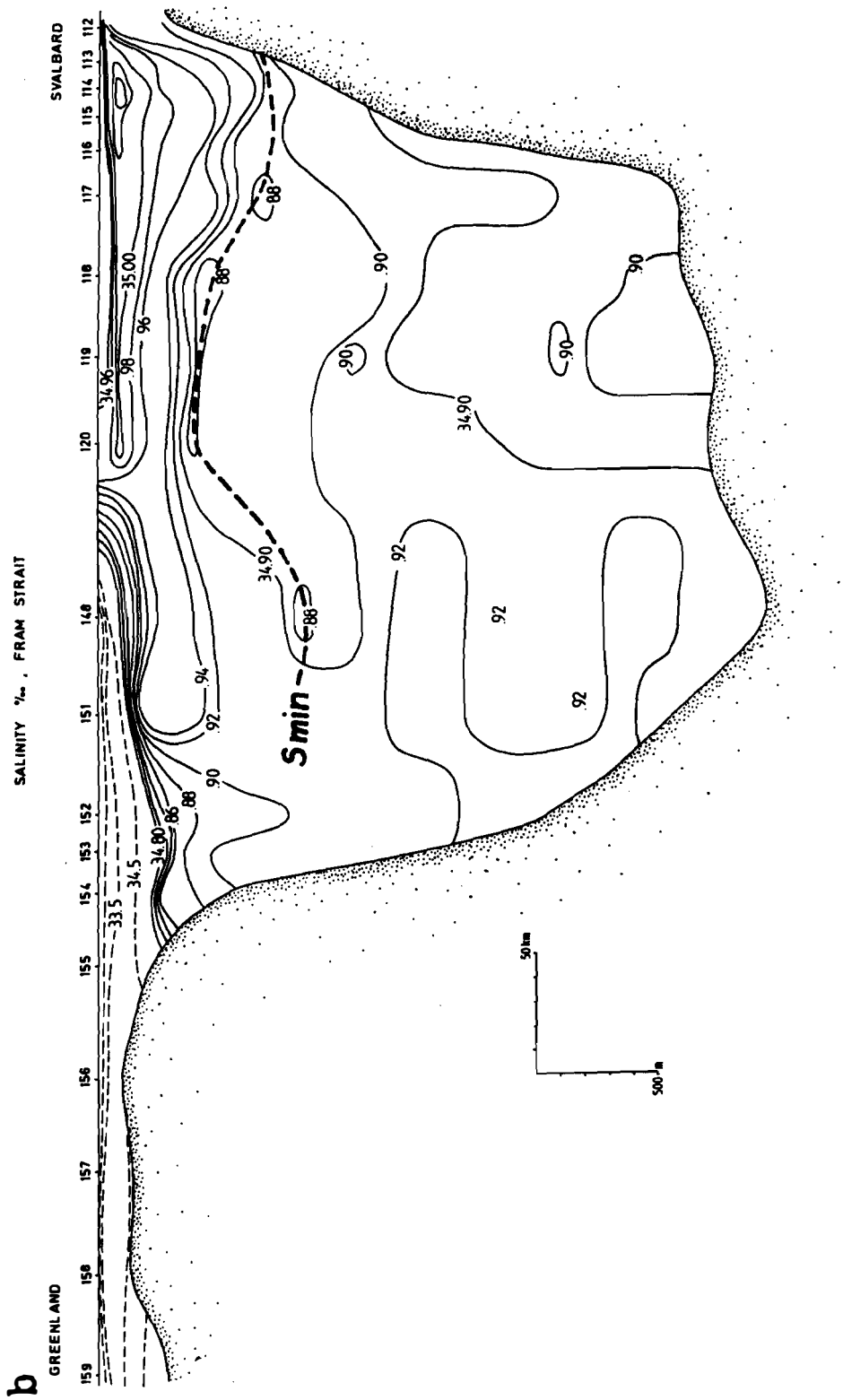
b
GREENLAND
SVALBARD
SALINITY ‰ , FRAM STRAIT
159 158 157 156 155 154 153 152 151 140 120 119 118 117 116 115 114 113 112
33.5
34.5
34.80
34.90
34.96
35.00
86
88
90
92
94
96
98
Smin
50km
500m

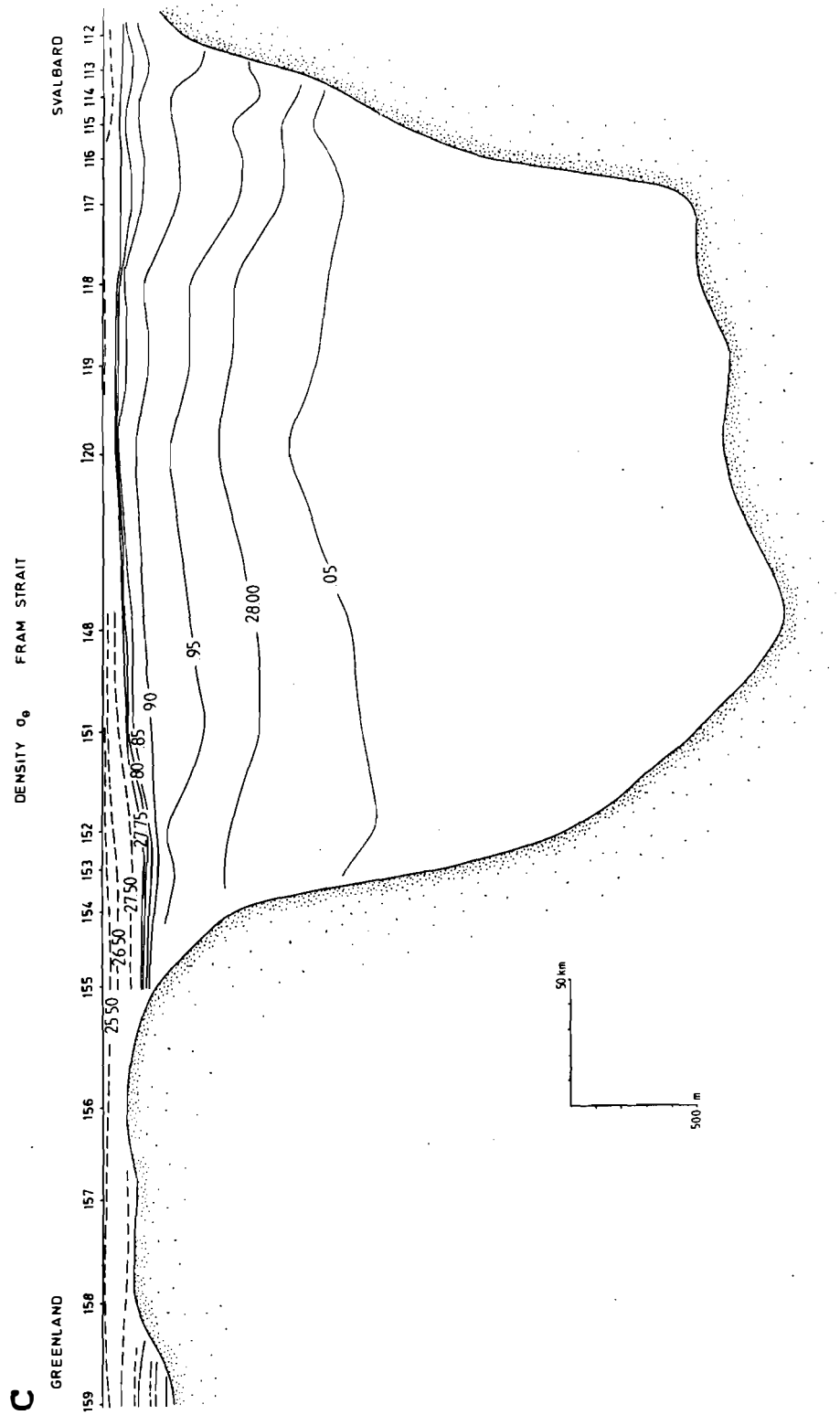
c
GREENLAND
SVALBARD
DENSITY σ_θ FRAM STRAIT
159 158 157 156 155 154 153 152 151 148 120 119 118 117 116 115 114 113 112
2550
2650
2750
2775
80
85
90
95
2800
05
50 km
500 m

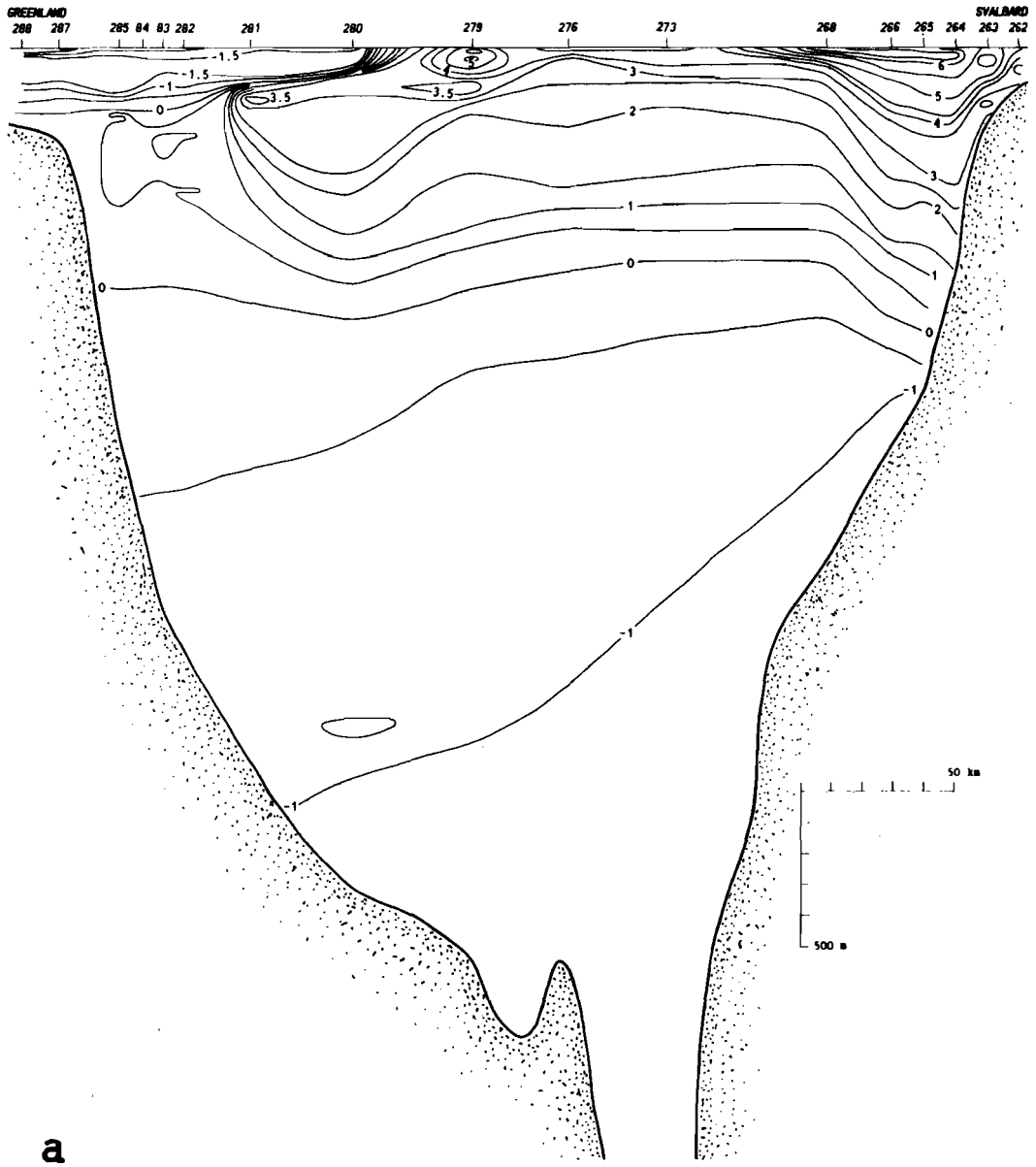

Figure 2a-c. Sections of potential temperature, salinity and potential density: LANCE section.

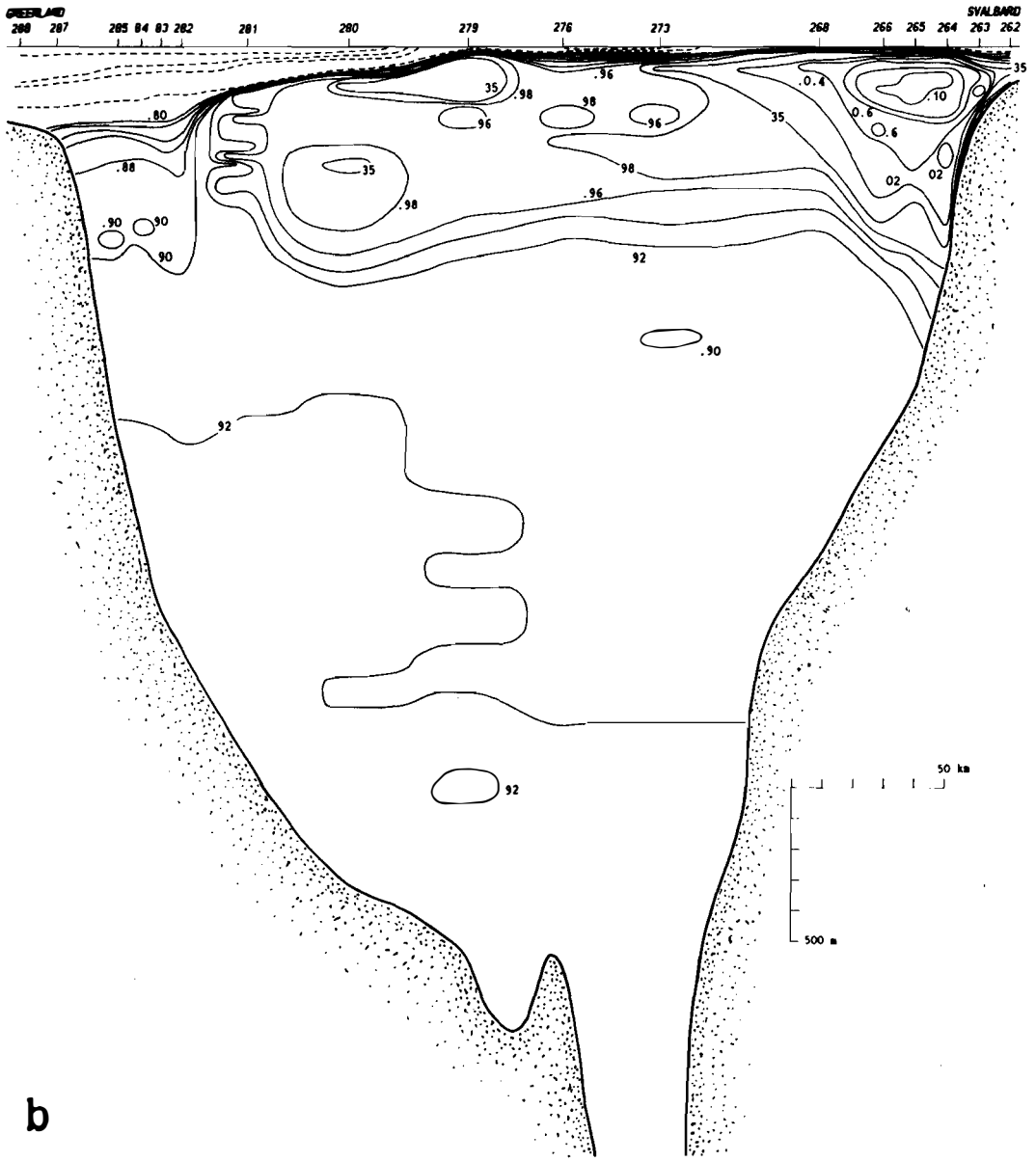
GREENLAND
288 287 285 84 83 282 281 280 279 276 273 268 266 265 264 263 262
SVALBARD
.80
.88
.90
.35
.98
.96
.92
.0.4
.10
.0.6
.02
50 km
500 m

b

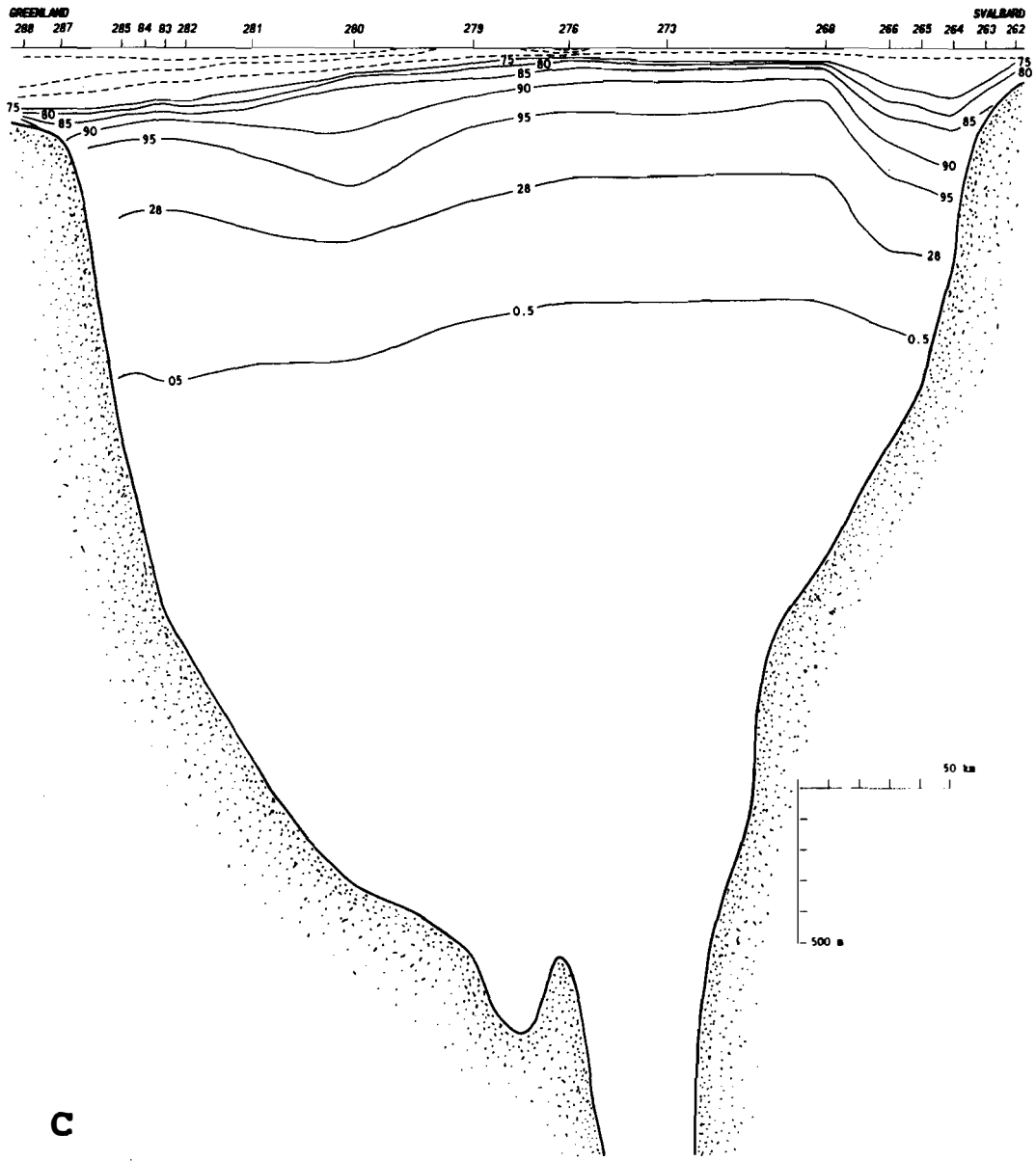
GREENLAND
SVALBARD
288 287 285 84 83 282 281 280 279 276 273 268 266 265 264 263 262
75
80
85
90
95
28
0.5
05
50 km
500 m

C

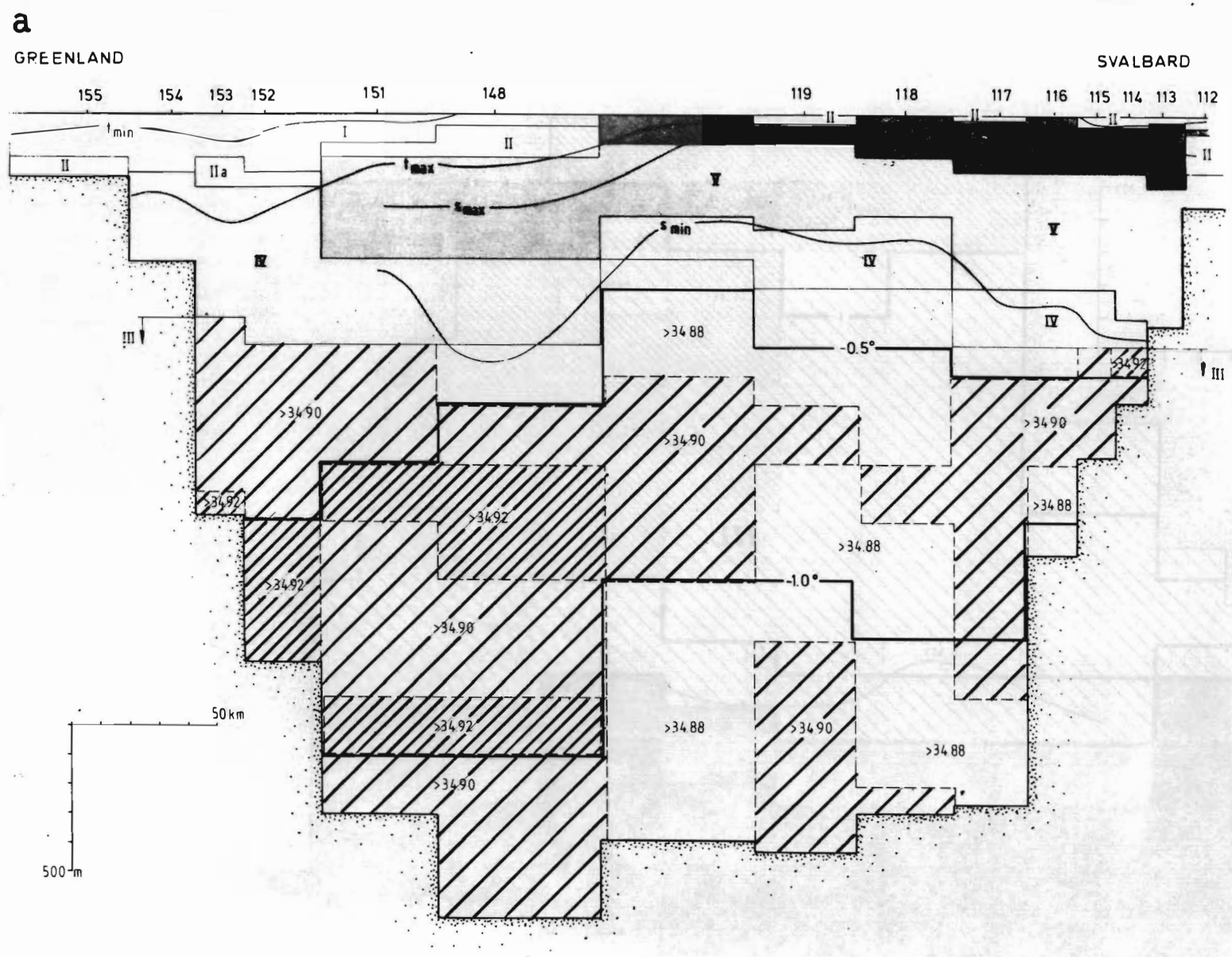

Figure 3a. The distribution of water masses I-VI on the YMER section.

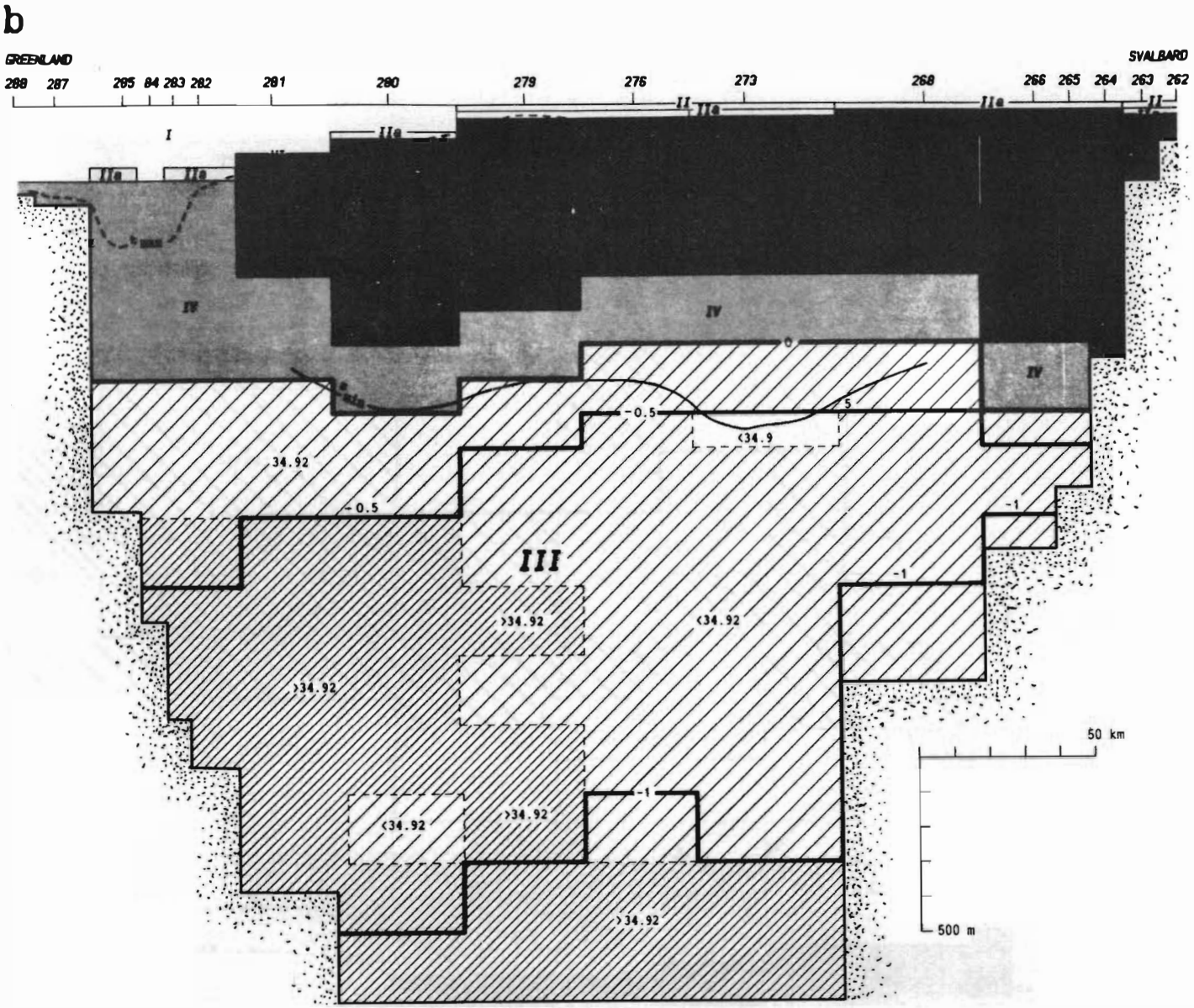

3b. The distribution of water masses I-VI on the LANCE section.

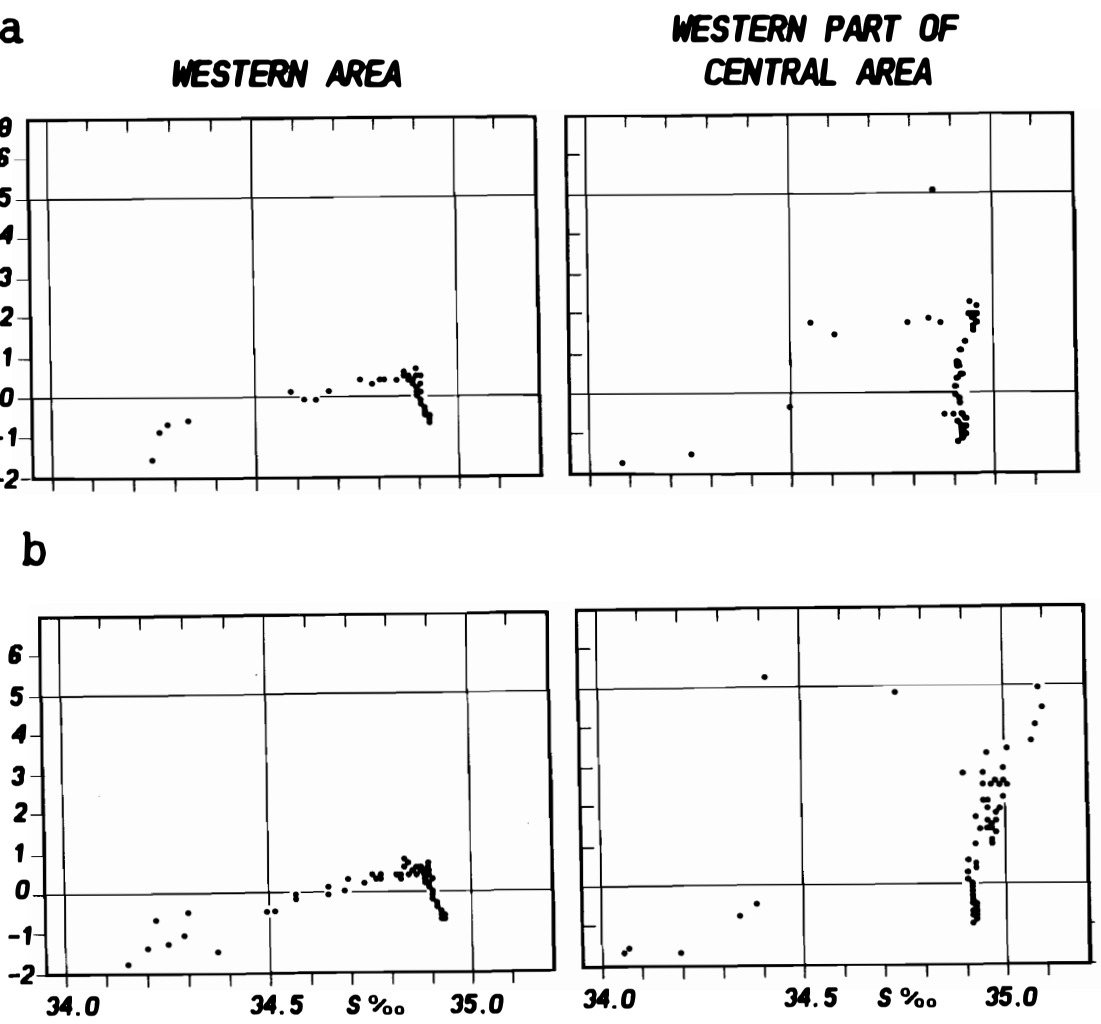

Figure 4a. θ-S diagrams for the YMER section.

a) eastern part, stations 112-116
b) central eastern part, stations 117-120
c) central western part, stations 148,151
d) western part, stations 152-155.

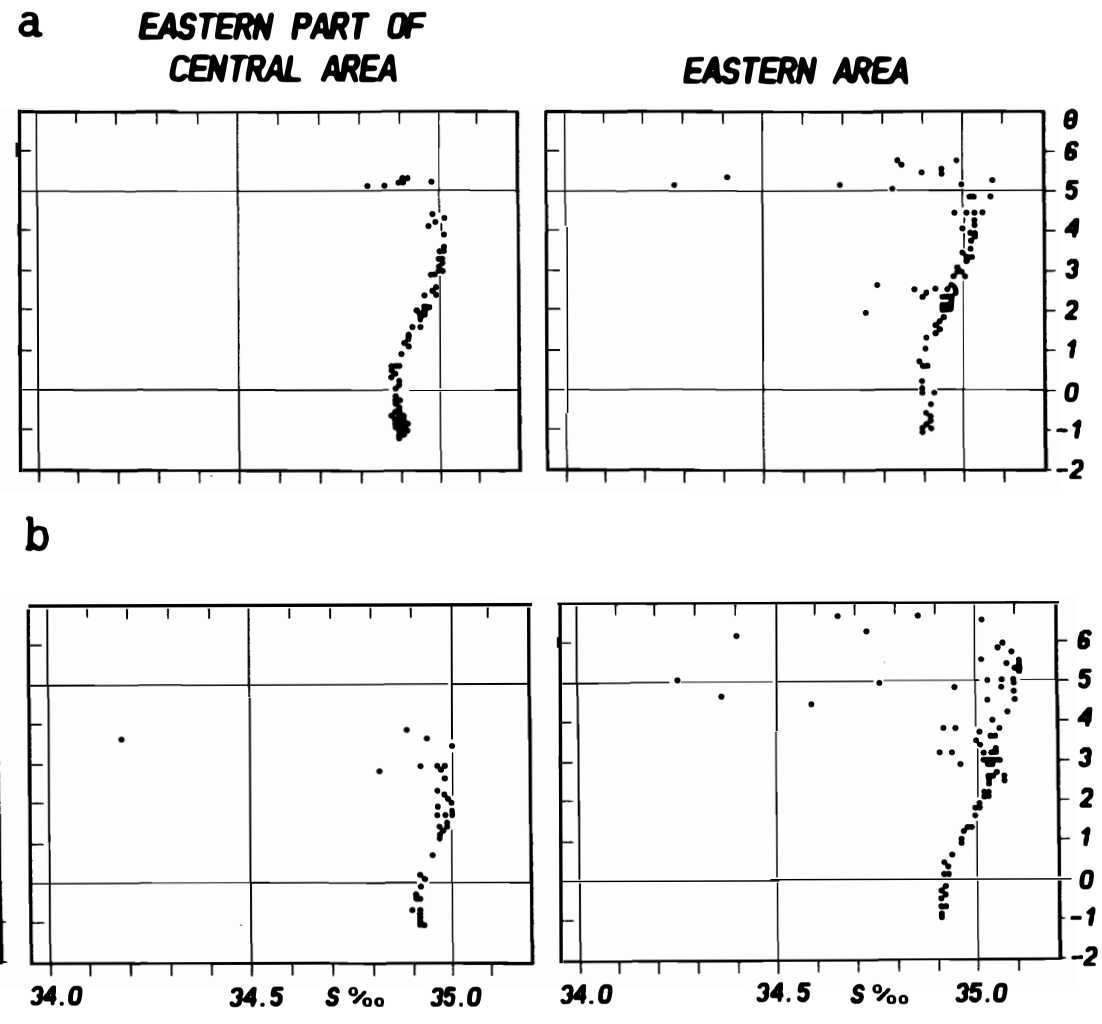

Figure 4b. θ-S diagrams for the LANCE section.

a) eastern part, stations 262-268
b) central eastern part, stations 273,276
c) central western part, stations 275-281
d) western part, stations 282-288.

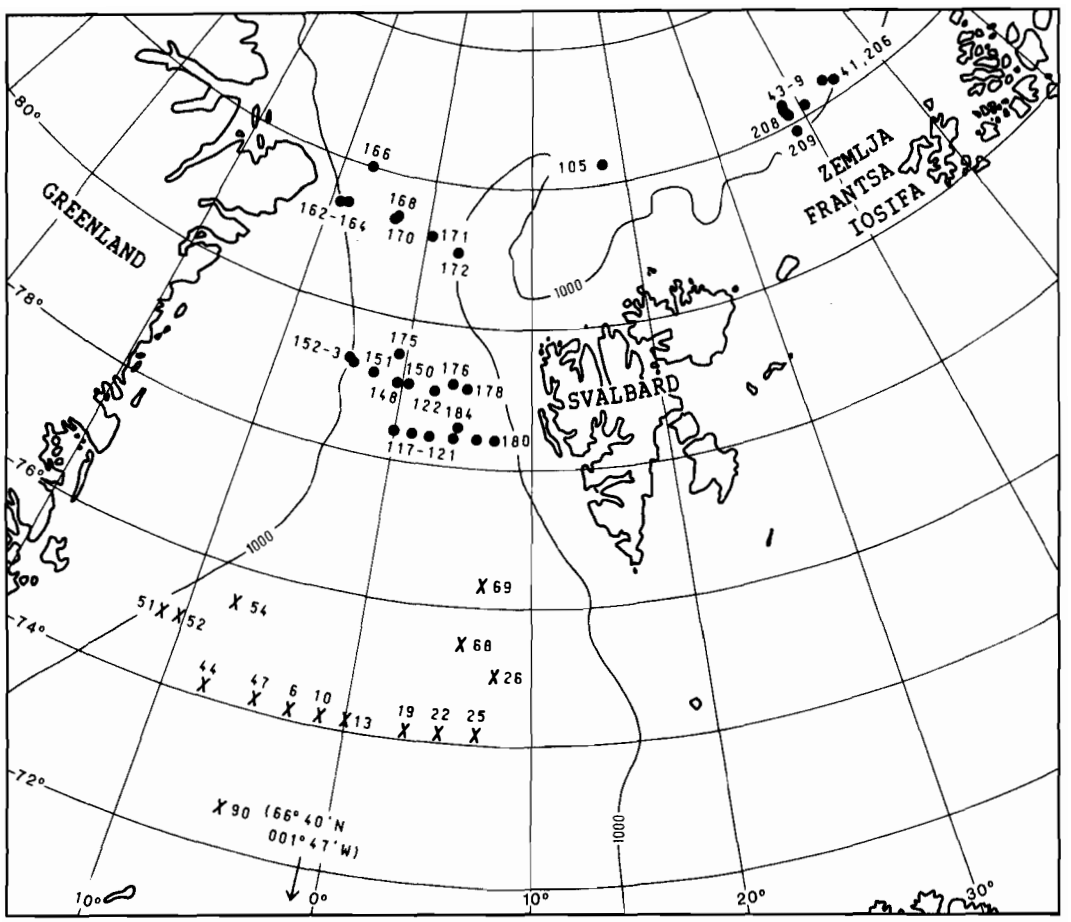

Figure 5. Chart showing the positions of the stations used in this work. Dots denote Polarsirkel and crosses Ymer stations.

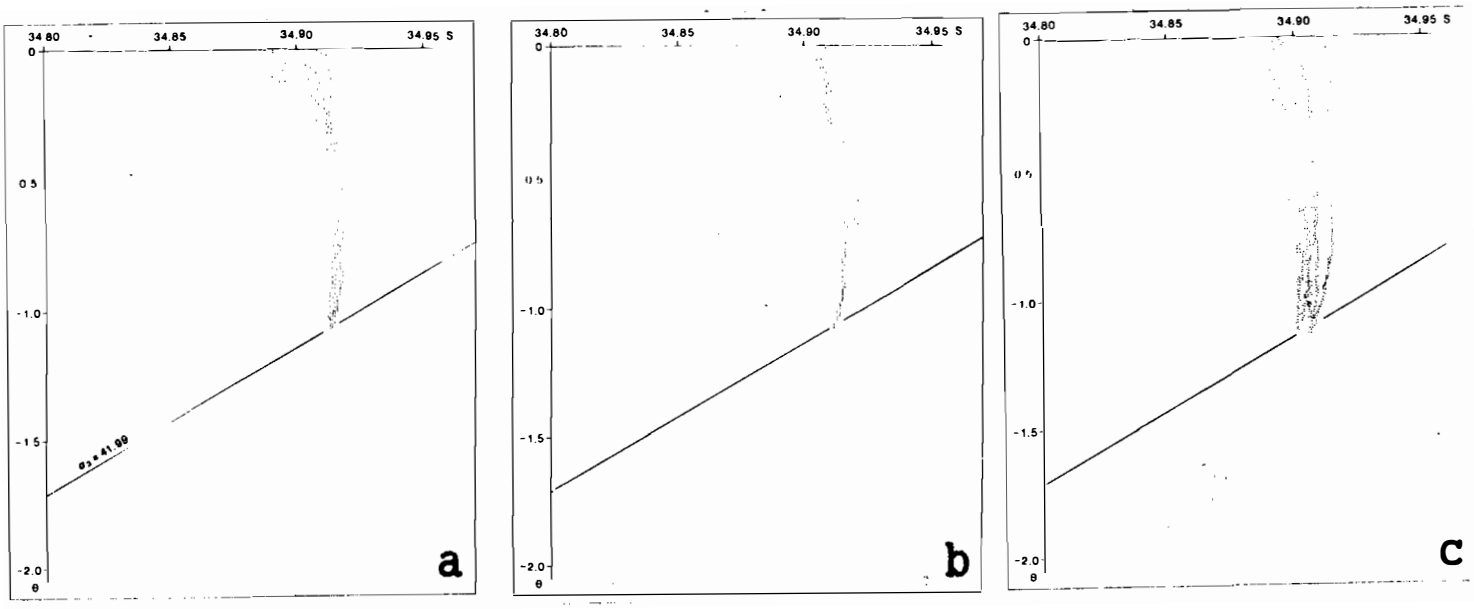

Figure 6a. θ-S curves from stations taken on the western slope of Svalbard. Station numbers Y-180, Y-183, Y-184.

Figure 6b. θ-S curves from stations taken on the western slope of the Yermak plateau. Station numbers Y-171, Y-172.

Figure 6c. θ-S curves from stations taken in the Norwegian Sea and in eastern part of the Greenland Sea, where Atlantic water is present in the upper layers. Station numbers P-25, P-26, P-68, P-69, P-90.

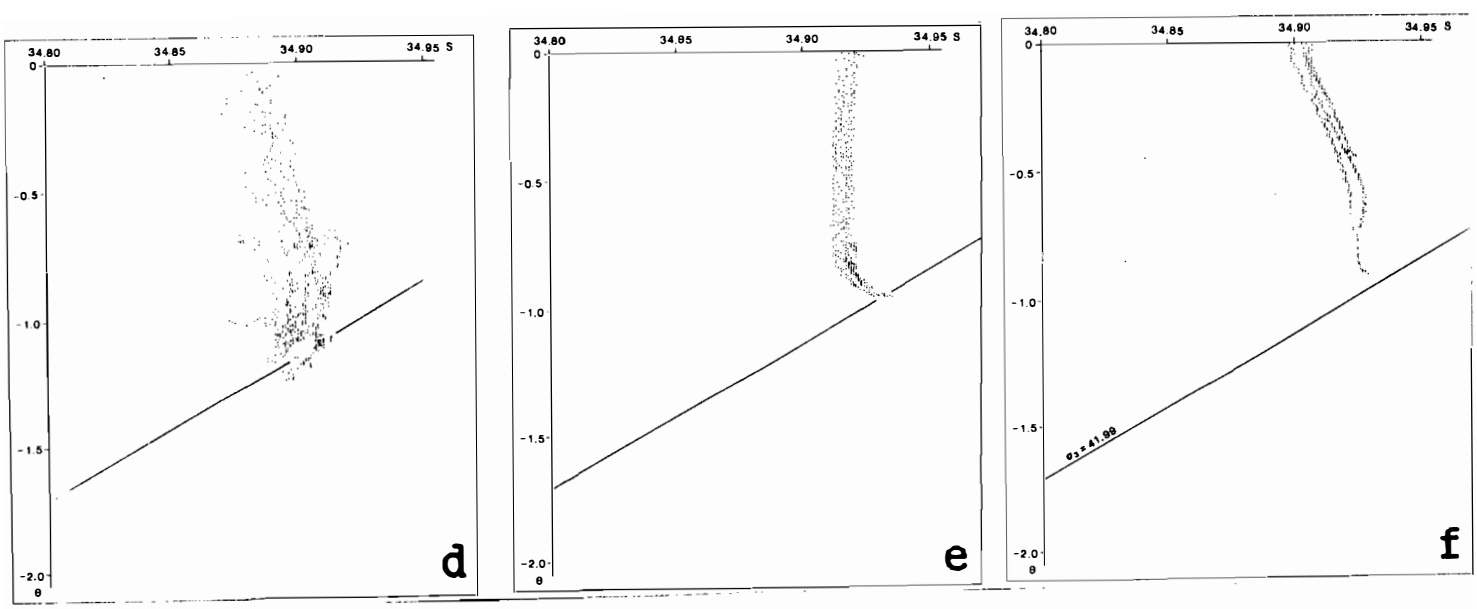

Figure 6d. θ-S curves from deep stations in the eastern part of Fram Strait. Station numbers Y-117, Y-118, Y-119, Y-120, Y-121.

Figure 6e. θ-S curves from stations taken north-west of Frans Josef Land. Station numbers Y-43, Y-44. Y-45, Y-46, Y-47, Y-48, Y-49, Y-50.

Figure 6f. θ-S curves from stations in the outflow area north-east of Greenland. Station numbers Y-152, Y-153, Y-162, Y-164.

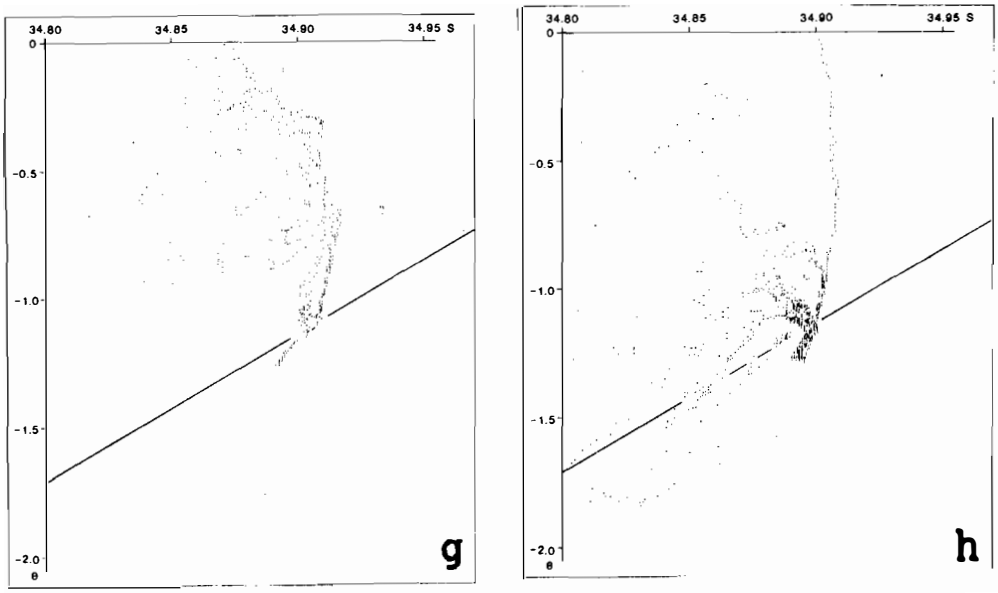

Figure 6g. θ-S curves from stations taken in the Greenland Sea on the continental slope. Station numbers P-52, P-53, P-54.

Figure 6h. θ-S curves from stations taken in different parts of the Greenland Sea. Stn. numbers P-8, P-10, P-13, P-22, P-25, P-44, P-47. The warm water is found on the most easterly stn. (P-25).

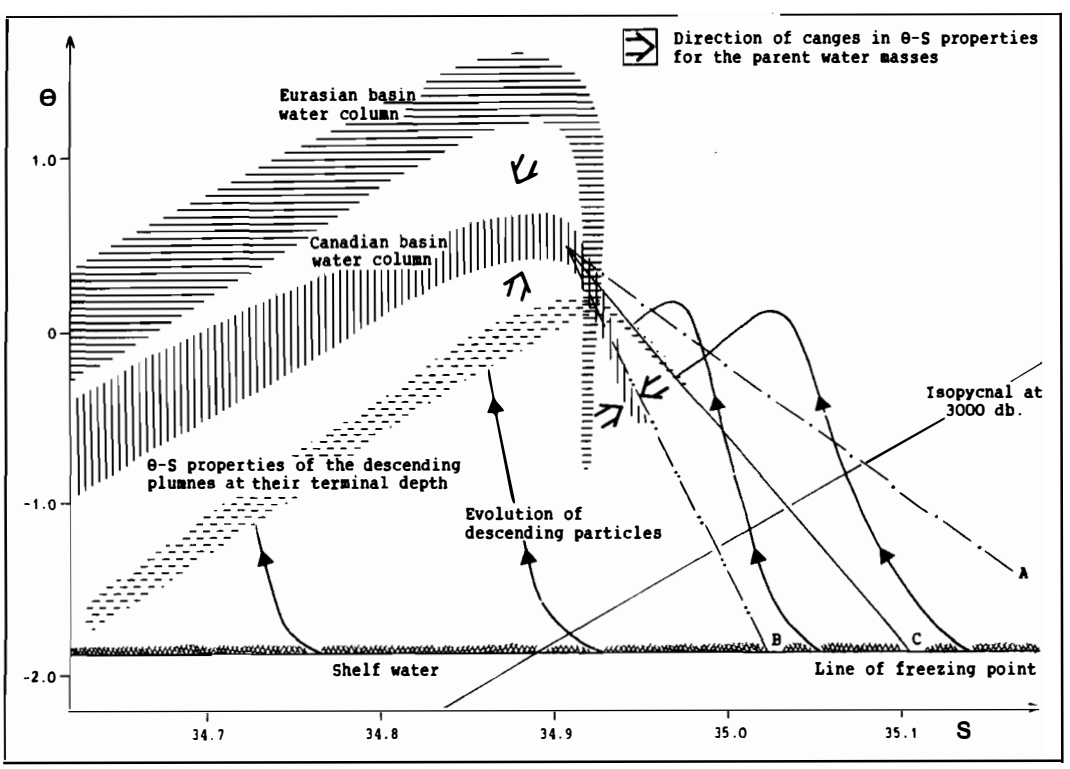

Figure 7. Transformation of Eurasian basin waters into Canadian basin waters. The water formed on the shelves lies along the freezing point line. For low salinities this water will, when it leaves the shelf, replenish the halocline. At higher salinities the water intrudes into and cools the Atlantic water, and may also become dense enough to enter the deep water. The evolution and final θ-S points for the descending plumes are sueggested. The ratio of the advective to convective contribution is taken to be 2:1.

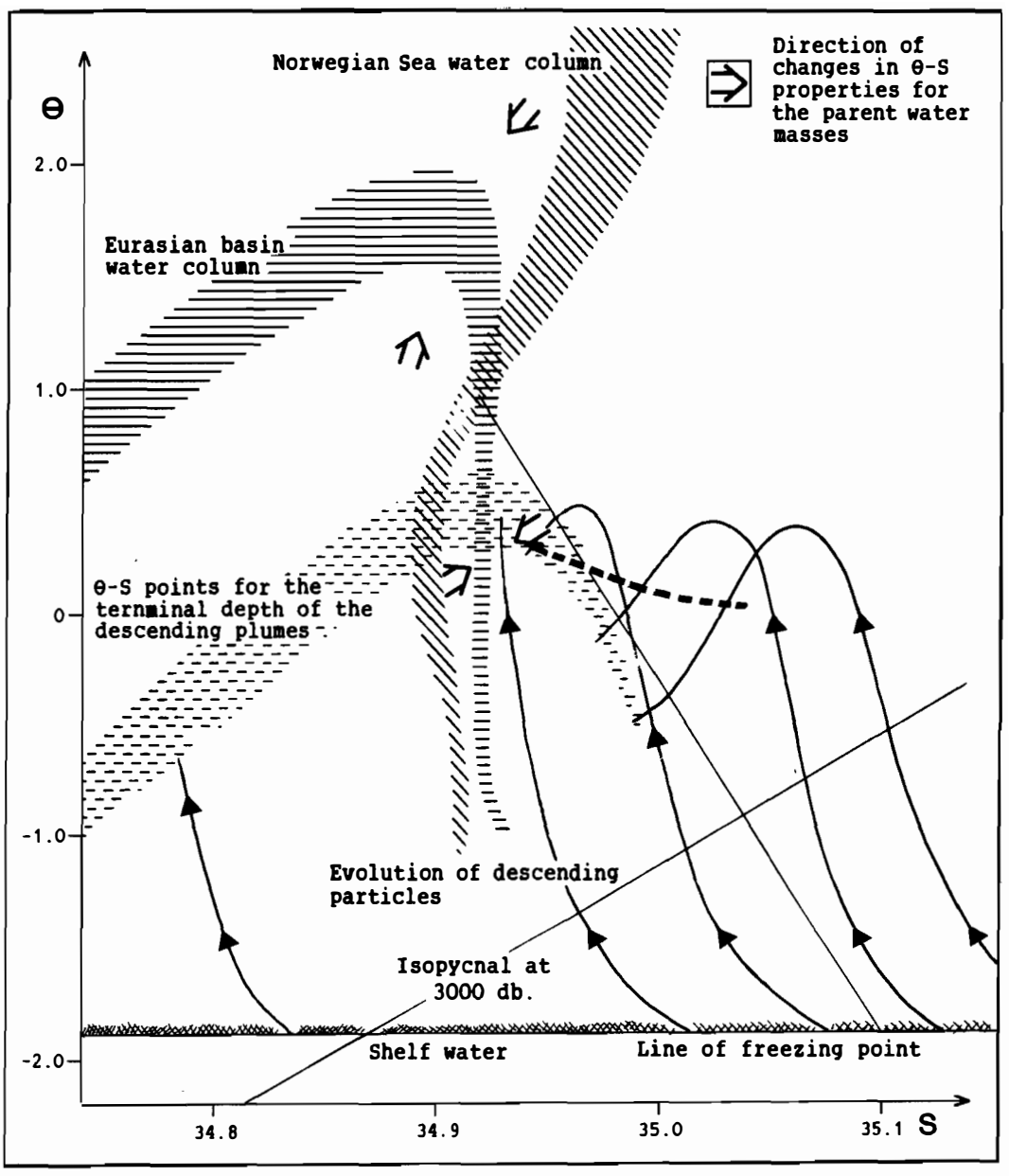

Figure 8. Transformation of inflowing Norwegian Sea and Greenland Sea waters into Eurasian basin waters. Broken line indicate when deep water begins to be entrained into the plumes. Assumed advective to convective contribution 8:1.

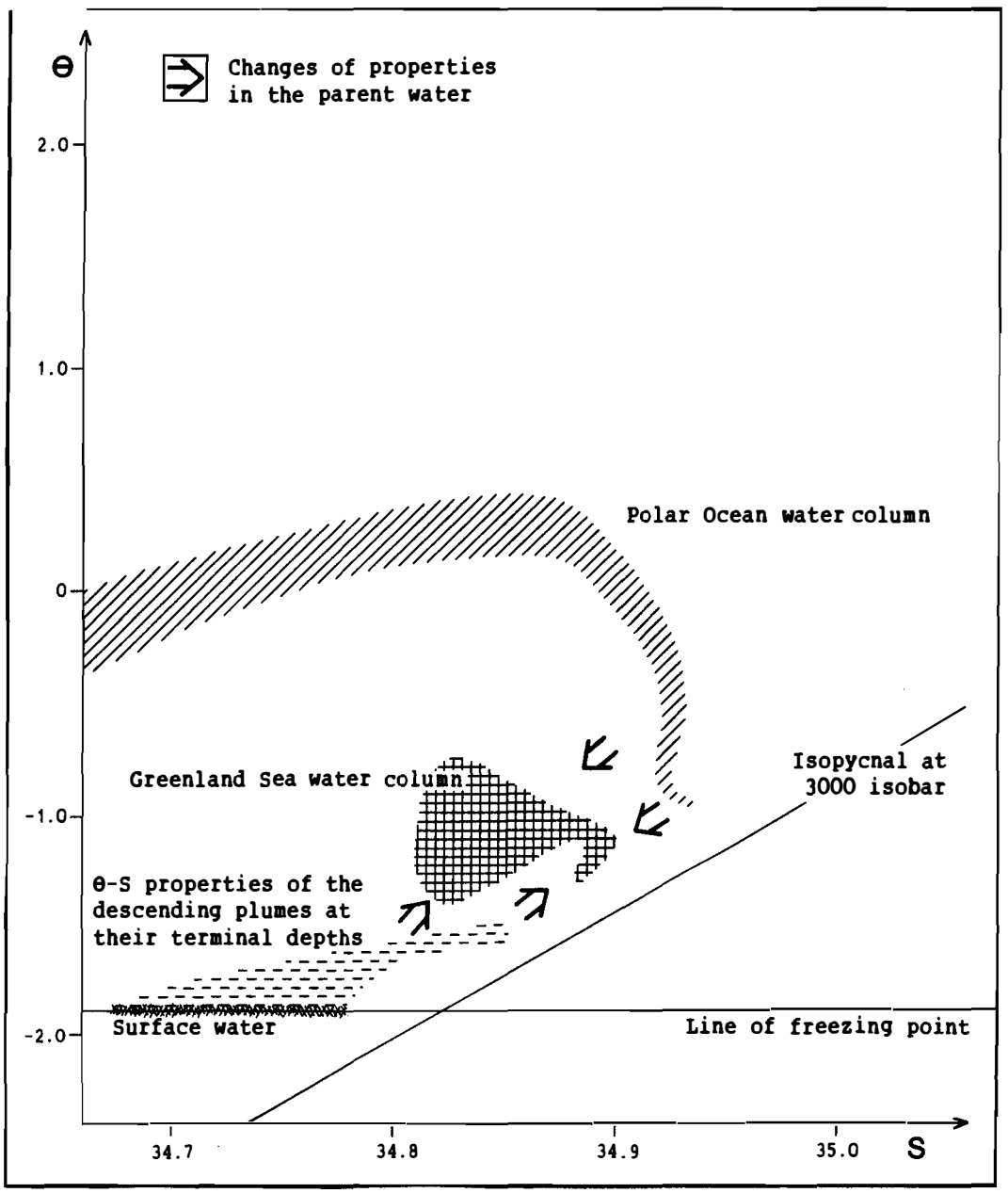

Figure 9. The formation of Greenland Sea deep water. Water cooled at the sea surface and made saline through ice formation sinks through the intermediate layers. The Surface and entrained water together with advected PODW maintain the θ-S structure of the Greenland Sea water column. The ratio of advected to convective contribution is rather arbitrarity taken to be 2:1.

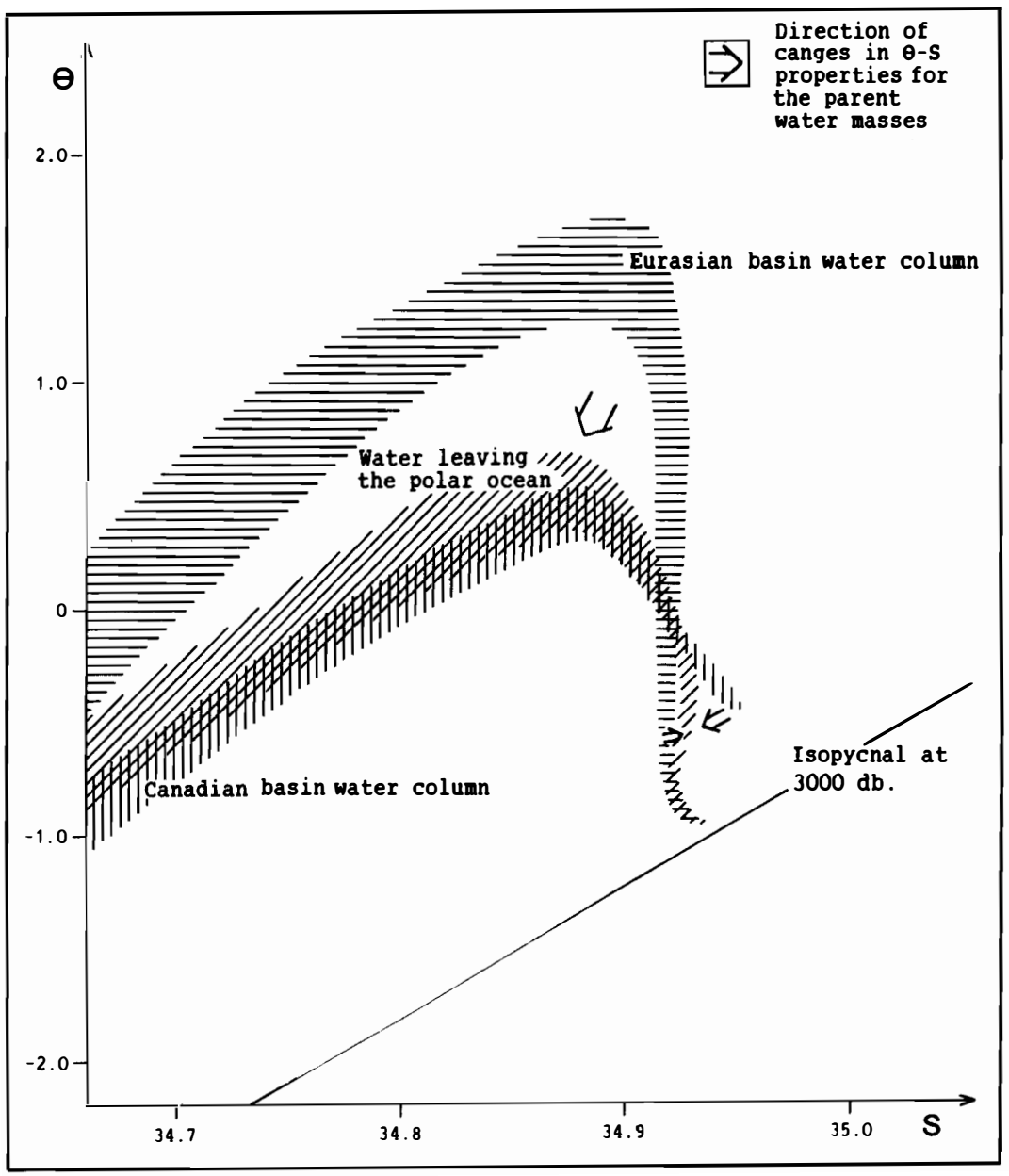

Figure 10. The waters from the Eurasian and the Canadian basins interacting to form the characteristics of the Polar outflow observed in the Fram Strait (surface layer excluded). Tentative ratio 2:1.

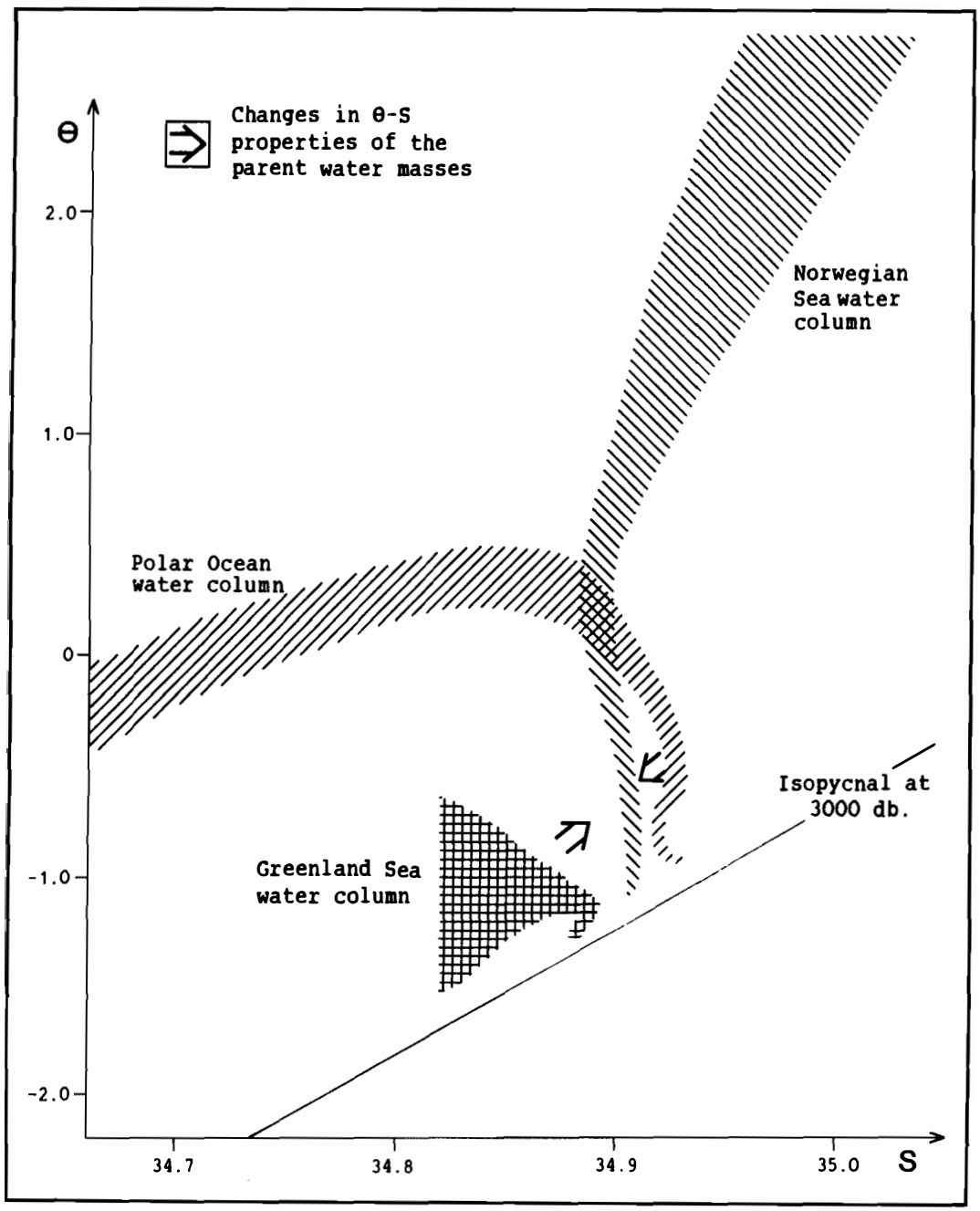

Figure 11. Formation of Norwegian Sea deep water trough isopycnal mixing of PODW and GSDW. The ratio between the water masses is tentatively put as 1:1.

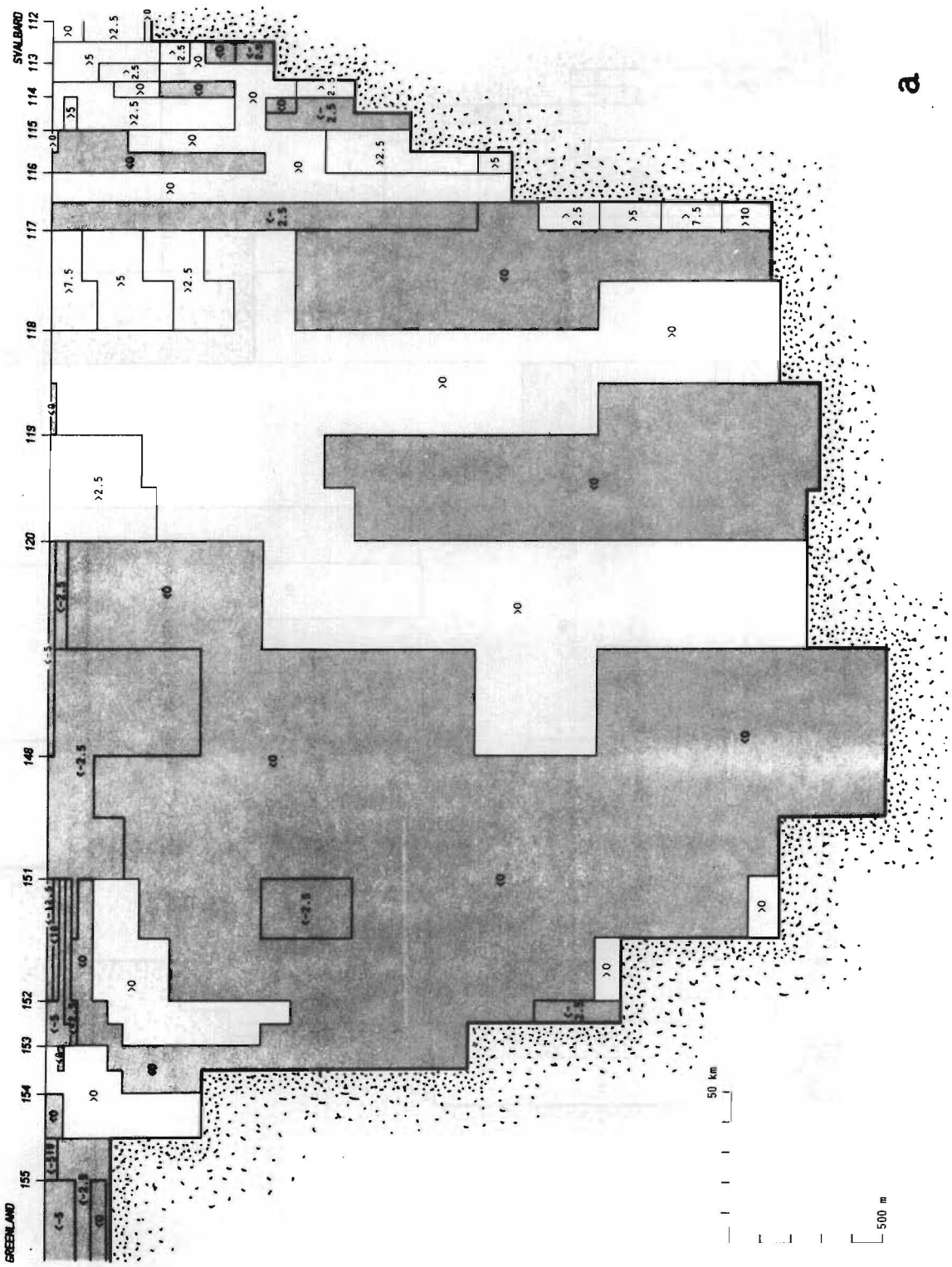

Figure 12. The velocity field in Fram Strait constraints on lower layer in addition to mass and salt continuity. Positive flow towards the north

a) YMER section.
b) LANCE section.

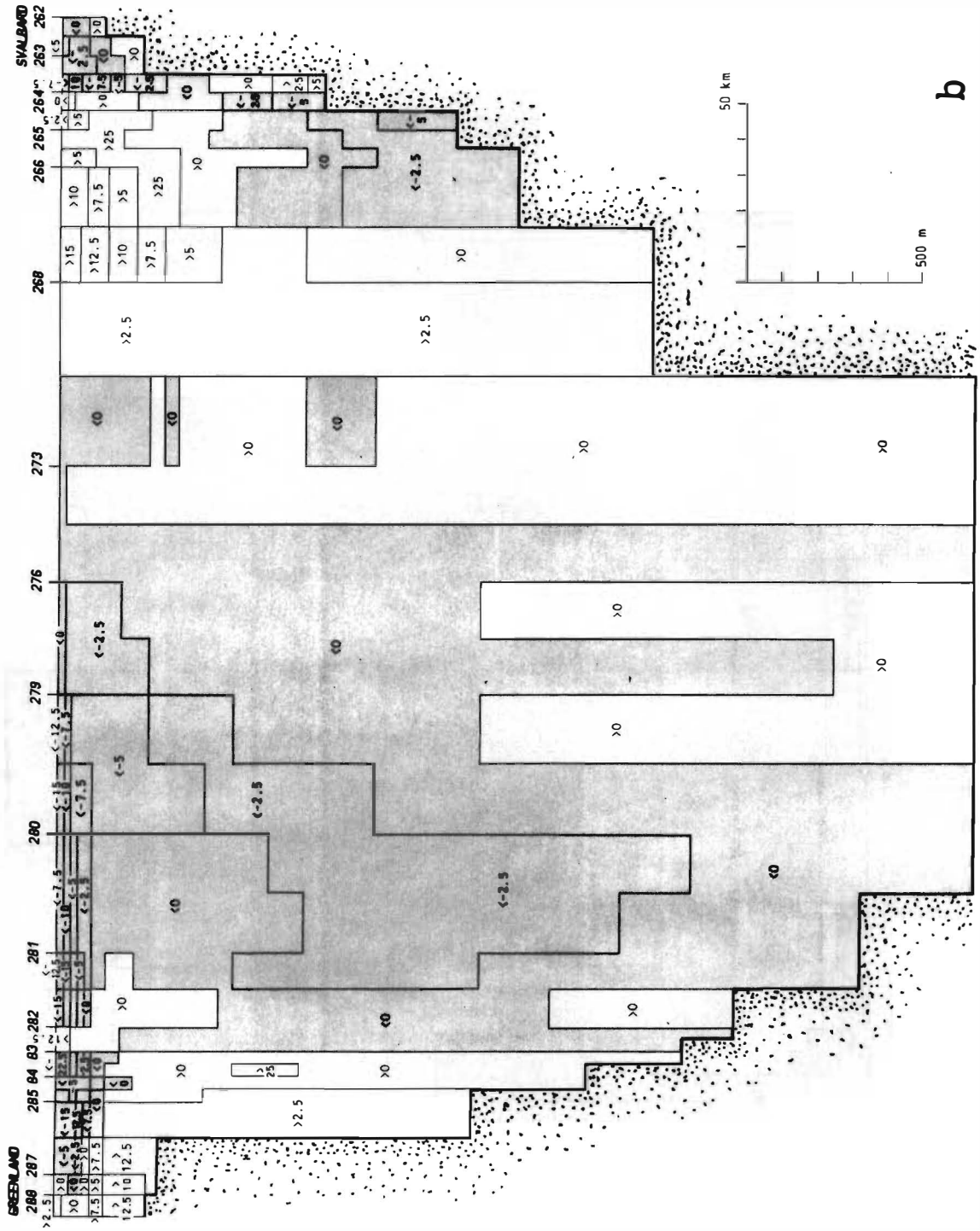
SVALBARD
GREENLAND
50 km
500 m
b

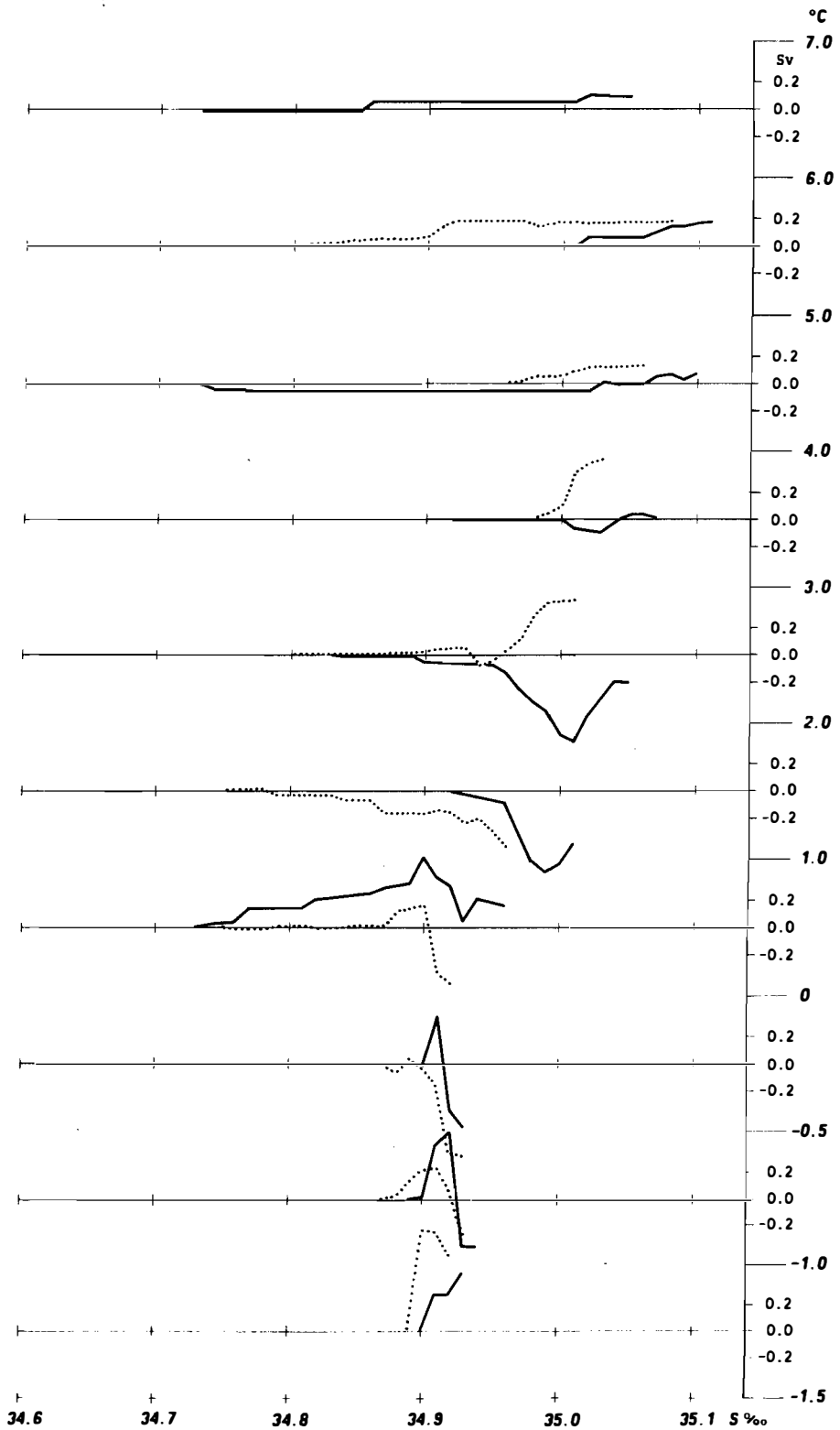

Figure 13. Integrated transports through the entire cross section in different temperature intervals as functions of salinity, S > 34.7.

Mass and salt continuity required and constraints on the deeper layers applied. Positive flow towards the north.

Dotted line: YMER section. Full line: LANCE section.

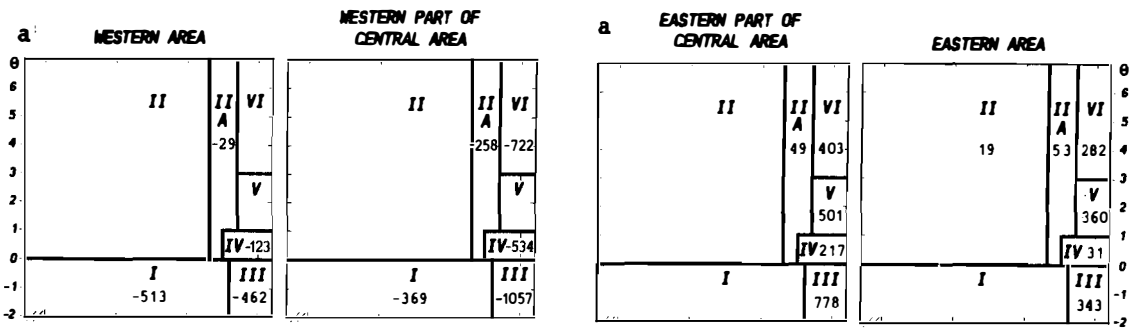

Figure 14a. Transports of different water masses through parts of the cross section.

Mass and salt continuity required and constraints on the deeper layers applied. Positive flow towards the north. YMER section.

a) eastern part
b) central part
c) central western part
d) western part.

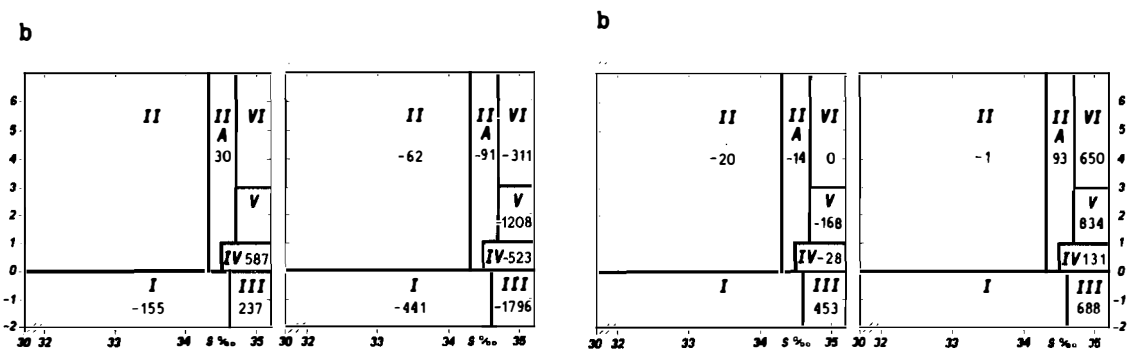

Figure 14b. Transports of different water masses through parts of the cross section.

Mass and salt continuity required and constraints applied on the deeper layers. Positive flow towards the north. LANCE section.

a) eastern part
b) central eastern part
c) central western part
d) western part.